Journal of Constructional Steel Research 207 (2023) 107956

Contents lists available at ScienceDirect

Journal of Constructional Steel Research

journal homepage: www.elsevier.com/locate/jcsr

Investigating the seismic performance of MRF-CBF dual systems under the effects of staged construction

Saeed Asil Gharebaghi *, Mostafa Ebad, Nader Fanaie

Faculty of Civil Engineering, K. N. Toosi University of Technology, Tehran, Iran

ARTICLE INFO

Keywords:
Staged construction analysis
Ordinary analysis
Column shortening
V braces
Invented-V (Chevron) braces
Split-X braces

ABSTRACT

In steel structures with moment-resisting frame-concentrically braced frame dual systems, as the moment-resisting frame can individually withstand gravity and seismic loads during construction, the braces can be installed on a story-by-story basis simultaneous with the installation of the moment frame or after its complete construction. This issue cannot be investigated and studied using ordinary analysis, where it is assumed that the entire structure is built at once, and then all the involved loads are applied to the completed structure. Accordingly, this research investigated the effects of staged construction in the mentioned dual systems with V, inverted-V (Chevron), and split-X braces. In this regard, three-dimensional models with 5, 10, 15, 20, and 25 stories incorporating these systems were generated and subjected to pushover analysis under cyclic loading protocols. From the results, it was concluded that staged construction could lead to maximum increases of 19.6% in the axial forces in internal columns due to dead load, 9.3% in the displacement corresponding to the first plastic hinge formation, 13.3% in the base shear corresponding to the first plastic hinge formation, 22.9% in the ultimate lateral strength, and 4.6% in the effective lateral stiffness. Also, staged construction was not found to significantly affect the axial forces in corner and braced-bay columns due to dead load and the energy dissipation under cyclic loading protocols.

1. Introduction

In the ordinary structural analysis method, gravity loads are applied to the structure after modeling the whole structure, while in reality, the structure is built in several different stages, where one story (as in concrete structures) or several stories (as in steel structures) are constructed in each stage. In such cases, the built stories of the structure are deformed under gravity loads, and new stories are placed on the deformed structure. The ultimate structure deformations are obtained from the sum of all deformations that occurred in each stage toward the structure's completion. Therefore, the assumed loads applied to the structure in the ordinary analysis do not match those in actual construction methods. Thus, the structure needs to be analyzed in each construction stage by considering the load changes corresponding to that stage. This method is known as staged construction analysis or construction sequence analysis (CSA) [1]. Figs. 1 and 2 schematically show the difference between ordinary and staged construction analysis. Staged construction analysis is a non-linear analysis method in which the structure is analyzed in different stages according to the construction stages, and the involved loads are applied to the structure in each stage [1].

Fig. 3 illustrates the steps in the staged construction analysis for a two-story structure. As seen in the figure, the first story is modeled in the first step. Then the loads corresponding to the first story are applied, and the structure's response is calculated. It should be noted that in concrete structures, which are outside the scope of this research, the deformations resulting from shrinkage and creep are also calculated based on concrete age and applied to the first story. The second story is modeled in the second step, and the related loads are subsequently assigned to that story. Ultimately, the response of the structure is calculated.

Column shortening is one of the most critical factors not considered due to the ordinary one-step design and neglecting step-by-step analysis. This issue causes a significant difference in the analysis results and causes the structure's capacity not to be fully used. In general, regardless of the structural system under assessment, the column shortening values in the one-step analysis follow an increasing trend along the structure's height. Nonetheless, in the staged construction analysis and with the gradual application of loads, the shortening values follow a significantly

* Corresponding author: Faculty of Civil Engineering, K. N. Toosi University of Technology, No. 1346, Valiasr St., P.O. Box 15875-4416, Tehran, Iran.
E-mail address: asil@kntu.ac.ir (S.A. Gharebaghi).

https://doi.org/10.1016/j.jcsr.2023.107956
Received 21 January 2023; Received in revised form 7 April 2023; Accepted 13 April 2023
Available online 26 April 2023

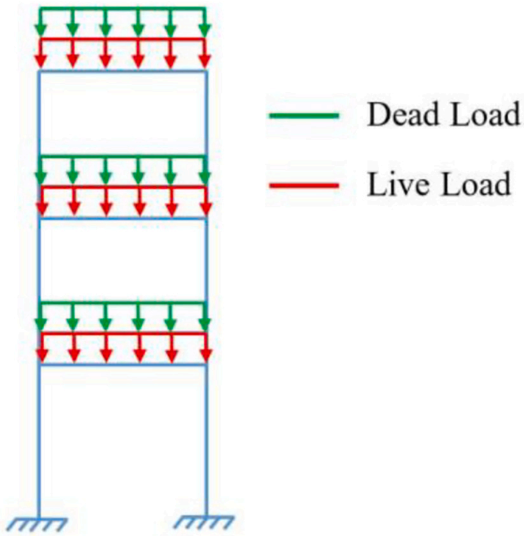

Fig. 1. Ordinary analysis (Adapted from [1]).

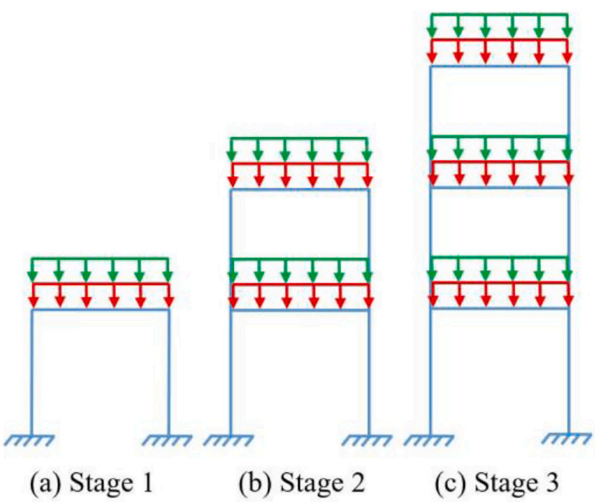

Fig. 2. Staged construction analysis (Adapted from [1]).

decreasing trend with the height, and the highest values occur in the middle stories of the structure (Fig. 4) [3].

Panigrahi et al. [1] evaluated the staged construction and ordinary analysis methods for three 20, 45, and 68-story reinforced concrete models in the ETABS software [4]. They studied the effect of staged construction on beam and column axial forces, shear forces, bending moments, and deflections. According to their results, the axial force in a floating column, supported by a load-bearing beam, increases by about 80% in the staged construction analysis compared to the ordinary analysis. They also found that in a column that continues to the foundation and is not floating, the staged construction analysis leads to an increase of about 30% in the axial force compared to the ordinary analysis. Also, they observed that the bending moment, shear force, and deformation of a transfer beam (on which a floating column is placed) increases by about 25% in the staged construction analysis compared to the ordinary analysis. Das and Praseeda [5] evaluated the staged construction and ordinary analyses for a 9-story commercial building. The investigated building was modeled in the ETABS software [4] to perform a staged construction analysis. Deflections, bending moments, and shear forces were investigated and studied in both of the analyses. In the ordinary analysis, dead, live, wind, and earthquake loads were applied simultaneously to the entire structure. From the comparison of the results, it was found that the deflections, bending moments, and shear forces from the ordinary analysis are less for the lower stories and more for the upper stories, compared to the values obtained from staged construction analysis. The effect of column shortening is also an important consideration in the design and construction of tall buildings, especially buildings with concrete or mixed systems. Rao et al. [6] compared the results of staged construction and ordinary analyses for a 24-story building in a Type III seismic zone. The analysis results were compared for a transfer beam and the frame above it. They observed a significant increase in loads and deflections in the staged construction analysis compared to the ordinary analysis. Amin and Mahajan [7] used the ETABS software [4] to study the results of staged construction analysis in multi-story buildings. They performed ordinary and staged construction analysis on three reinforced concrete buildings with 5, 7, and 9 stories. Their research investigated parameters such as bending moments, axial and shear forces, and deflections under earthquake and wind loads using both analysis methods. It was concluded that staged construction analysis is necessary for improving the accuracy of the analysis in terms of deflections, axial forces, bending moments, and shear forces in transfer beams and their adjacent columns, as well as the whole structure, for reinforced concrete and steel structures. Shirhatti and Vanakudre [8] investigated the effects of linear static, time-dependent, and staged construction analyses for reinforced concrete and steel structures. Six three-dimensional (3D) models with 5, 10, 15, 20, 25, and 30 stories were modeled in the ETABS software [4] for each reinforced concrete and steel building. This research found that staged construction significantly increases the shear forces and bending moments in beams with floating columns. Paranay et al. [9] and Jagarlamudi and Manoj [10] investigated a 22-story building with floating columns and transfer beams through ordinary and staged construction analyses in the ETABS software [4]. They concluded that for multi-story buildings with floating columns and transfer beams, it is necessary to consider the effects of staged construction. Dinar et al. [2] analyzed three-dimensional reinforced concrete and steel frames with different configurations based on staged construction. The time-dependent effects of creep, shrinkage, concrete stiffness change, and step-by-step loading were considered to analyze 12 three-dimensional models. The results showed that staged construction causes a significant increase in bending moment, shear force, and deflection of a beam with floating columns, and this increase reduces with the decrease in the number of stories. Pathan et al. [11] analyzed numerous reinforced concrete frames with different span numbers and lengths, story heights, and story numbers using the STAAD.Pro software using ordinary and staged construction methods. They concluded that staged construction analysis is critical even if the earthquake forces are ignored in the construction stages. Choi et al. [3] investigated the effects of sequential gravity loads on two models, one with 60 steel stories and another with ten reinforced concrete stories (with and without shear walls). Numerical simulation of these two high-rise buildings confirmed the importance of the differential column shortening effect. The results showed that the differential column shortening and the bending moments induced by this effect are significant in the gravity analysis of the entire frame and should not be ignored in the analysis of tall buildings. The corresponding column shortening values were also presented in figures similar to Fig. 4.

Moment-resisting frame-concentrically braced frame (MRF-CBF) dual systems are a structural solution for high-rise buildings, combining the strength and ductility of both systems. Several studies have focused on various topics related to such systems. Rodríguez et al. [12] presented a sensitivity and fragility analysis of steel MRFs featuring top-and-seat with web angle connections under progressive collapse scenarios. Wijesundara et al. [13] evaluated the seismic performance of suspended zipper concentric braced frames, a type of MRF-CBF dual system designed to improve the performance of conventional concentric braced frames. Mazzotta et al. [14] presented the design and verification steps of tall steel frame structures with braced core, belt, and outrigger trusses, comparing the results of response spectrum analysis and nonlinear time history analysis in terms of seismic response. Wijesundara et al. [15] investigated the seismic performance of brace-beam-column connections in concentrically braced frames, evaluating the strength and deformation capacity of the connections and their sensitivity to design parameters.

In steel structures with MRF-CBF dual systems, since the moment frame can individually withstand gravity and seismic loads during construction, the braces can be installed on a story-by-story basis simultaneous with the installation of the moment frame or after its complete construction. Accordingly, this research studies the effects of staged construction on MRF-CBF dual systems. Also, while investigating the column shortening phenomenon and the column axial forces, the seismic performance of MRF-CBF dual systems is evaluated.

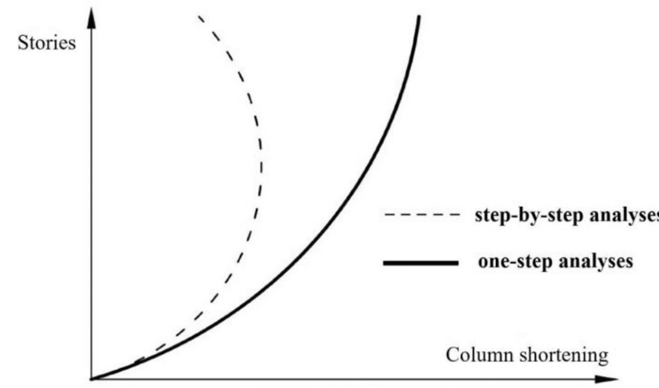

Fig. 4. Column shortening under step-by-step and one-step analyses [3].

2. Modeling and ordinary design of the considered 3D MRF-CBF dual systems

Fifteen 3D models of 5, 10, 15, 20, and 25 stories with MRF-CBF dual systems with V, inverted-V (Chevron), and split-X braces were evaluated in this study. They were modeled and ordinarily designed per the assumptions discussed in the following:

2.1. Structural systems and floor plan

The structural systems used for the models under consideration were the intermediate moment frame (IMF) and the special concentrically braced frame (SCBF) for gravity and lateral load-bearing systems, respectively. The floor plan for all models was identical, with three 5-m bays in both the *X*- and *Y*-directions, as shown in Fig. 5. Moreover, all stories had a uniform height of 3 m. Braces were installed in the middle bay of the external frames in both the *X*- and *Y*-directions, as illustrated in Fig. 6. The direction of the floor slab beams was modeled with a checkerboard pattern since the lateral load-bearing system was the same in both directions.

2.2. Materials and loading conditions

The steel type used in all models was the S235JR steel. Additionally, box sections were used for columns, European rolled I-sections and, where necessary, built-up I-sections were used for beams, and double-channel sections were used for braces. The models were loaded according to ASCE7–16 [16] provisions, with the dead and live floor loads considered as 600 kg/m^2 and 200 kg/m^2, respectively. The construction site was assumed to have high seismicity with type-B soil.

2.3. Design code and seismic design requirements

The AISC360–10 design code [17] was used to design all models. In addition, the seismic design requirements for concentrically braced frames included in the AISC341–10 provisions [18] were observed in designing all the MRF-CBF dual systems evaluated in this study.

3. Staged construction analysis of the designed models

In this paper, three construction models were examined. The first

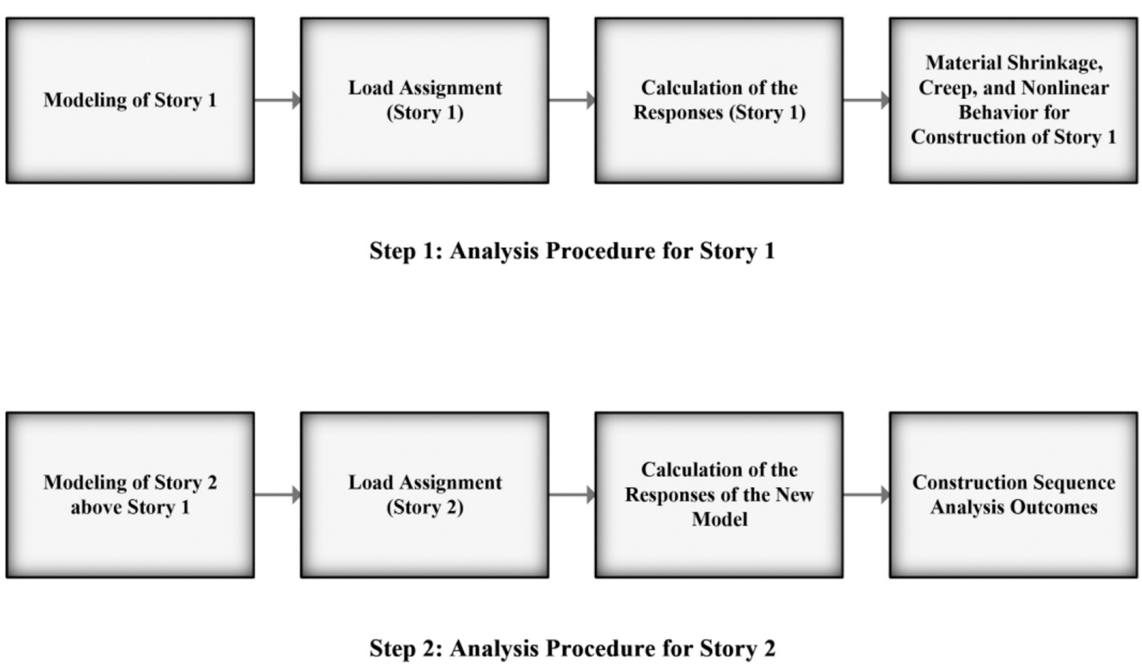

Fig. 3. The steps in staged construction analysis for a two-story structure (Adapted from [2]).

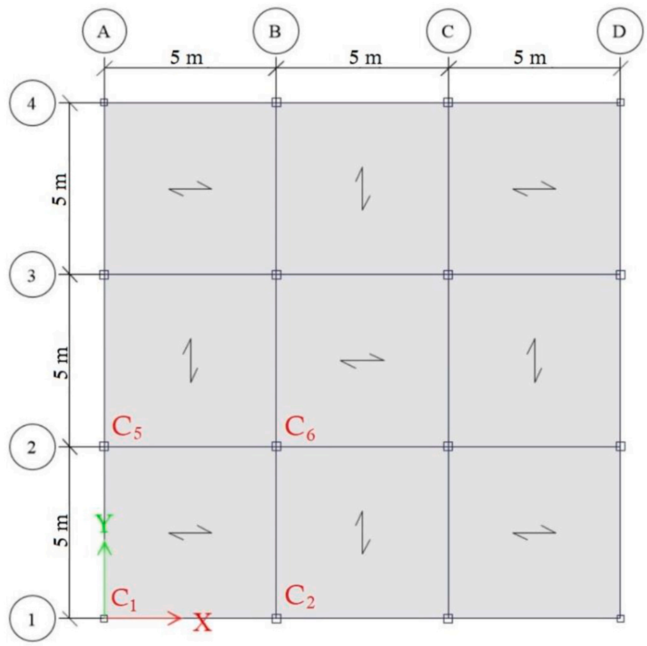

Fig. 5. The typical floor plan of the models and positions of the evaluated columns.

model is the ordinary one, where it is assumed that the entire structure is built instantaneously in one step, and the gravity and lateral loads are applied to the complete structure. Considering that a structure with an MRF-CBF dual system can bear the gravity and seismic loads during the construction before installing the braces through the moment frame, based on the construction method of such structures, two staged construction models defined as in the following were also examined:

a) Staged construction model I, where one story with braces is built in each stage.
b) Staged construction model II, where one story without braces is built in each stage, and the braces are installed in the last stage.

It should be noted that in defining the staged construction models, only the dead gravity loads of the structure are applied to the models in each stage.

4. Pushover analysis of the designed models

In order to assess the designed models' seismic parameters and the effects of staged construction on them, pushover analyses were conducted for all generated models and in three cases of the ordinary model and staged construction models I and II.

According to FEMA 356 [19], in the method of non-linear static analysis, termed pushover analysis, the lateral seismic load is applied to the structure in a static and gradually increasing manner. The pushover analysis continues until the displacement at a certain point (control point) under the effect of lateral load reaches a specific value (target displacement) or the structure collapses. In this research, the center of mass of the structure's roof was considered as the control point.

Based on FEMA 356 [19] provisions, the lateral load distribution in the pushover analysis can be considered in different ways. In this paper, the uniform pattern, where the lateral load is calculated per the weight of each story, was utilized. In order to investigate other methods of lateral load distribution, pushover analyses with a pattern corresponding to the shape of the first mode and an inverted triangle pattern were also performed in the 5- and 25-story models.

The beams in the braced bays were load-bearing in the models with V, inverted-V (Chevron), and split-X braces in the X direction. Hence, due to gravity loads, tensile and compressive axial forces would be induced in V and inverted-V (Chevron) braces, respectively. Therefore, to more closely examine the models with the braces mentioned above, pushover analysis was performed in both X and Y directions.

Using the center of mass displacement versus base shear curve, termed the pushover curve or the capacity curve, the displacement and base shear values corresponding to the first plastic hinge formation and the ultimate lateral strength of the structure were calculated. Furthermore, using the bilinear behavior model for the pushover curve, as displayed in Fig. 7, the displacement and base shear values corresponding to the yield point of the models were extracted. Subsequently, the models' effective lateral stiffness (K_e) values were calculated according to Eq. (1).

$$K_e = \frac{V_y}{\delta_y} \tag{1}$$

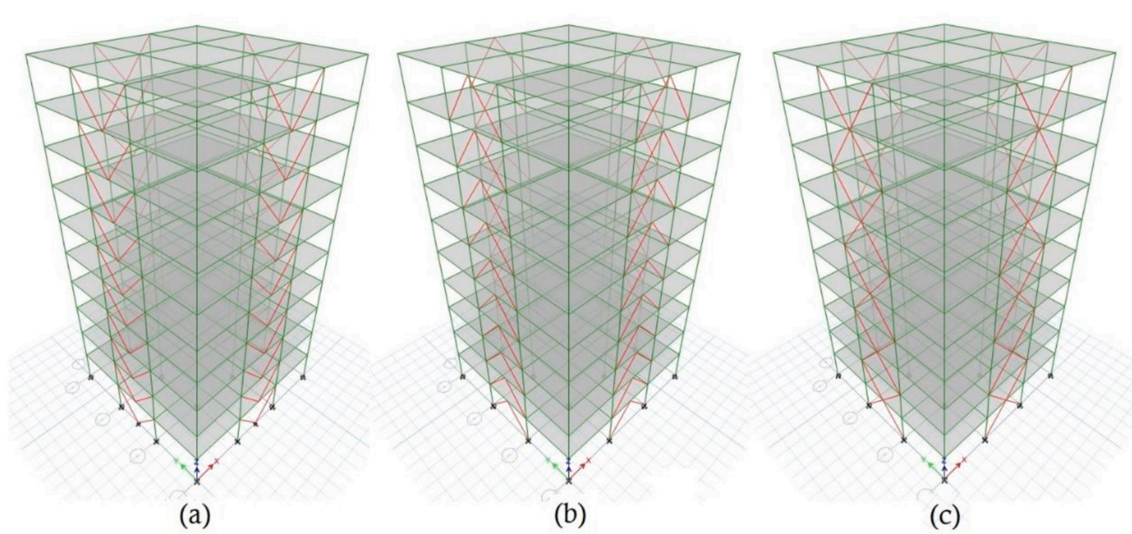

Fig. 6. The designed 10-story models: (a) V concentric braces; (b) Inverted-V (Chevron) concentric braces; (c) Split-X concentric braces.

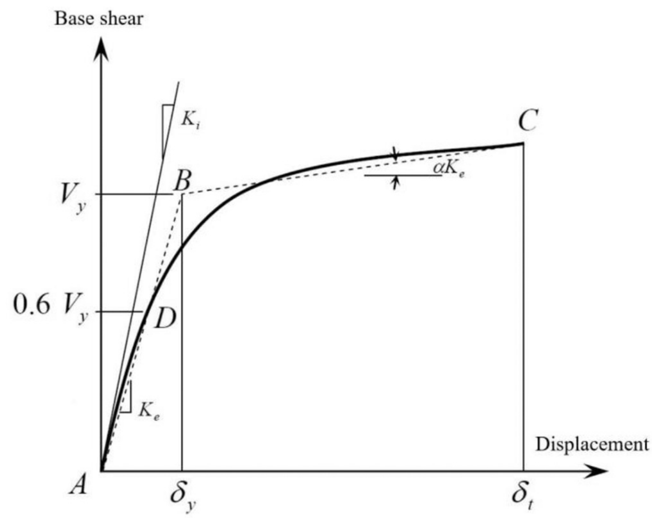

Fig. 7. Bilinear model for the pushover curve.

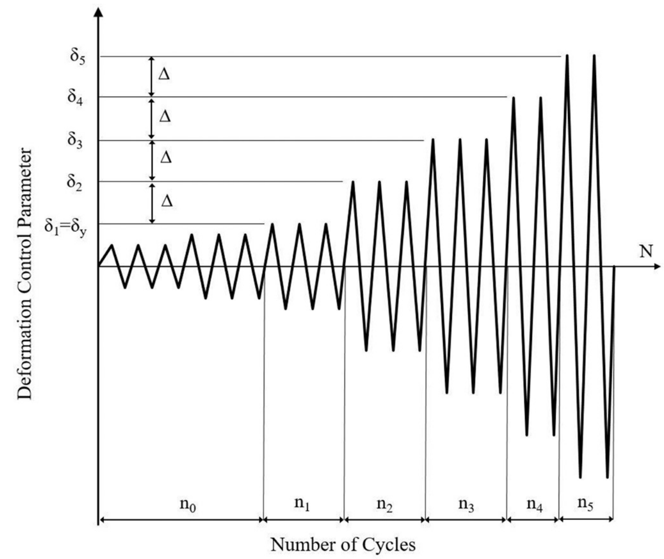

Fig. 9. The ATC-24 cyclic loading protocol [20].

5. Application of the cyclic loading protocol and extraction of the hysteresis curves of the designed models

To investigate the effects of staged construction on the hysteresis curves of the models and to investigate and compare the amount of energy dissipated in the models, all models were subjected to cyclic loading protocols. For this purpose, the AISC 341–10 [18] and ATC-24 [20] cyclic loading protocols, as illustrated respectively in Figs. 8 and 9 were used.

Since cyclic loading protocols are mainly used to generate the hysteresis curves of one-story structures or beam-to-column connections, the cyclic loading protocol in this research was utilized according to Panyakapo's paper [21] as follows:

In order to calculate the desired amount of drift in the loading protocol, the lateral displacement of the roof level (Δ_h) was divided by the structure's total height (*H*). For example, to apply a drift of 0.01 in the 25-story model, the structure's roof level was subjected to a displacement of 75 cm.

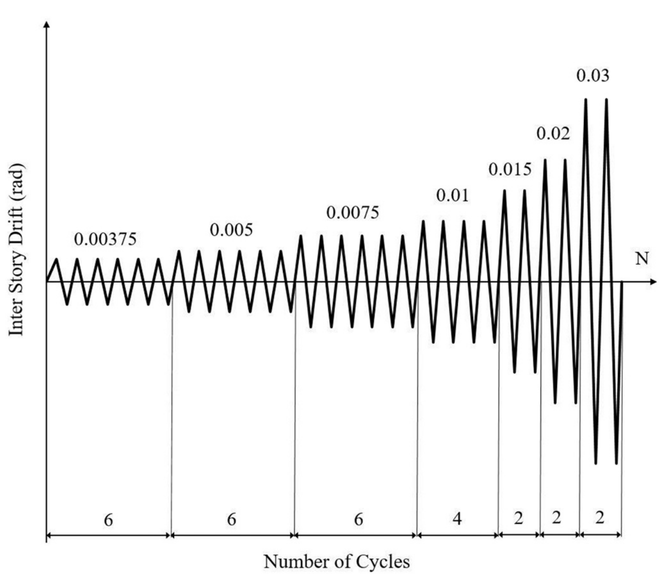

Fig. 8. The AISC 341–10 cyclic loading protocol [18].

$$\text{Drift} = \frac{\Delta_h}{H} = \frac{75}{25 \times 300} = 0.01 \quad (2)$$

Using the bilinear behavior model for the pushover curve according to Fig. 7, the yield displacement value *(δ_y)* was extracted for each model.

6. Presentation and interpretation of the values obtained for column axial forces due to dead load

This section investigates the effect of staged construction on column axial forces due to dead load. Fig. 10 shows the graphs of the column axial forces by story number in the 25-story model with inverted-V (Chevron) braces as an example. Also, Fig. 11 shows the graphs of the column axial force changes for an internal column in the first story (C_6) in the models with the inverted-V (Chevron) braces. As can be seen from the results presented in Tables 1 to 3, the effect of staged construction on the axial forces caused by dead load is insignificant and can be ignored in corner columns (C_1), braced-bay columns with load-bearing beams (C_2), and braced-bay columns with non-load-bearing beams (C_5). Also, in most models, staged construction leads to reduced values for axial forces resulting from dead load in the mentioned columns, which can be considered in the direction of reliability.

According to the results given in Table 4, in an internal column (C_6), staged construction increases the axial force caused by dead load up to about 19.6%. An interesting point worth mentioning is the difference between the axial forces caused by dead load in staged construction model I (one story with braces in each stage) and staged construction model II (one story without braces in each stage and installation of all braces in the last stage) is very small. This shows that the increase in the axial force caused by dead load in an internal column is primarily affected by the overall staged construction process, and the sequence of installing the braces has an insignificant effect on this increase. Therefore, when the effects of staged construction are not considered, the design force corresponding to an internal column is estimated to be less than the actual amount. Such an issue leads to incorrect design, which can be dangerous. In order to study the impact of staged construction on the design of an internal column, the internal columns of the first, second and third stories of the 25-story model with split-X braces were investigated on a case-by-case basis. The demand-to-capacity ratios (DCRs) of the mentioned columns under the critical design load combination (including gravity and seismic loads) in the ordinary model were calculated as 0.810, 0.828, and 0.752, respectively. The DCRs for

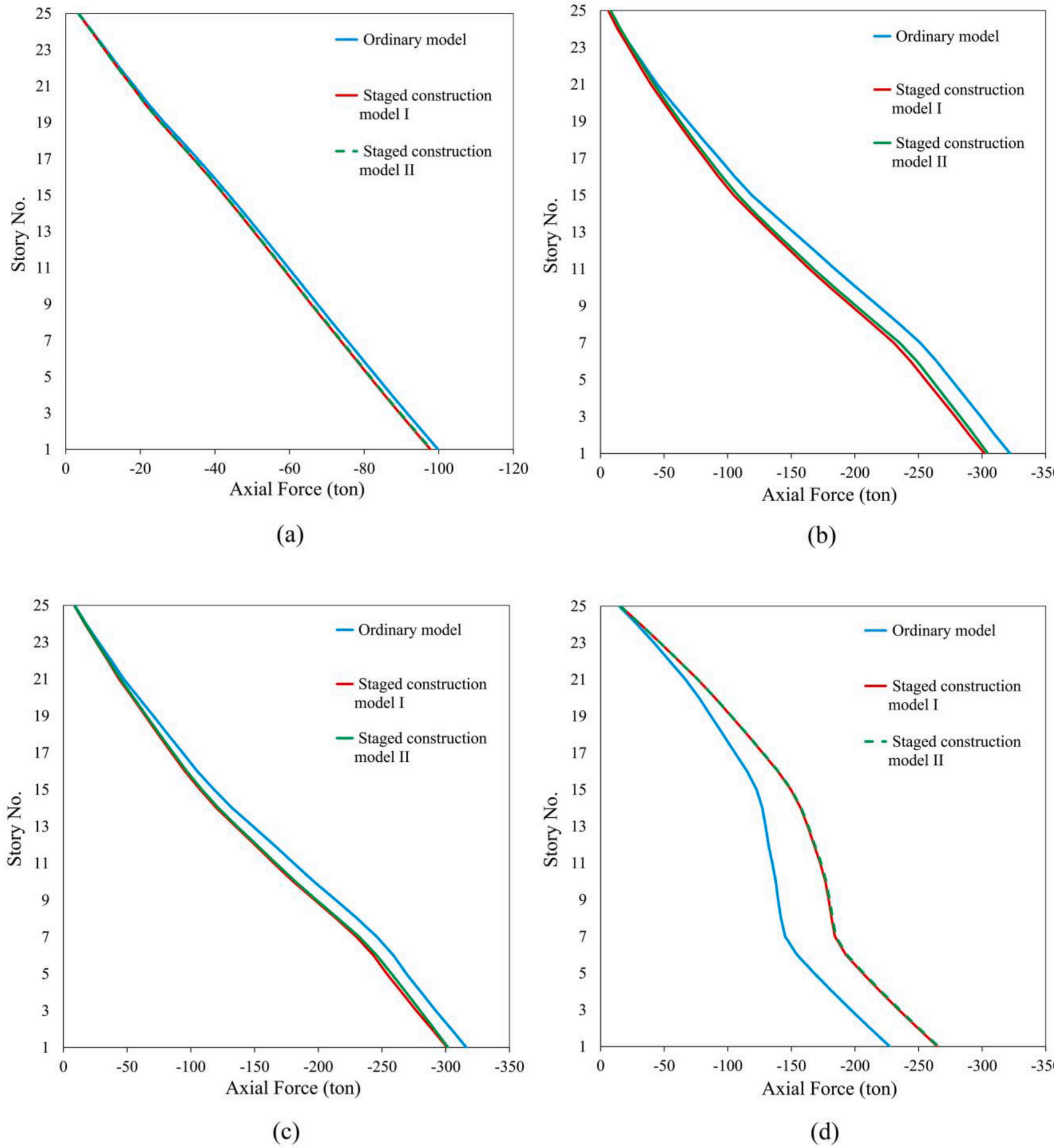

Fig. 10. Graphs of the axial forces in the columns due to dead load versus story number in the 25-story model with inverted-V (Chevron) braces: (a) Corner column (C_1); (b) Braced-bay column with load-bearing beam (C_2); (c) Braced-bay column with non-load-bearing beam (C_5); (d) Internal column (C_6).

the columns mentioned above under the critical design load combination in staged construction model II were also calculated as 0.908, 0.956, and 0.888, respectively. The above calculations show that the staged construction process in the 25-story model with split-X braces caused increases of about 12%, 15%, and 18% in the DCRs for the internal columns of the first, second, and third stories, respectively, which is significant.

It can be observed that the amount of increase in the aforementioned axial forces decreases with the decrease in the number of stories. Also, the most significant increase in the axial force caused by dead load in an internal column (C_6) due to the effects of staged construction occurs in the model with the split-X braces, followed by the models with inverted-V (Chevron) and V braces, respectively.

As mentioned earlier, the increase in axial force caused by dead load

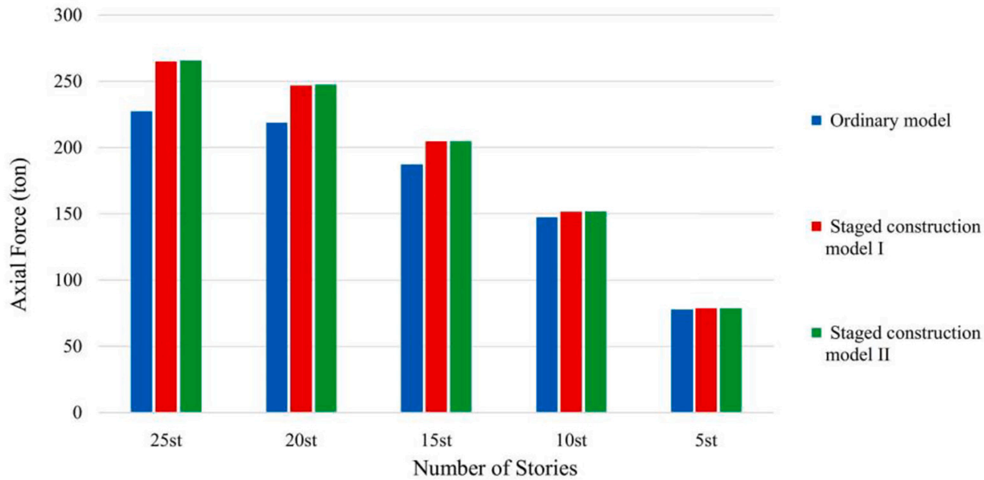

Fig. 11. Graphs of the column axial force changes for an internal column in the first story (C_6) in the models with the inverted-V (Chevron) braces.

Table 1
Results for the axial force due to dead load in a corner column (C_1) and the changes compared to the ordinary model.

Story	Model	Column axial force - C_1 (ton)					
		V braces		Inverted-V (Chevron) braces		Split-X braces	
	Ordinary model	17.81	0.0%	18.06	0.0%	17.86	0.0%
5	Staged construction model I	17.38	−2.4%	17.76	−1.6%	17.58	−1.6%
	Staged construction model II	17.40	−2.3%	17.75	−1.7%	17.60	−1.5%
	Ordinary model	34.58	0.0%	34.42	0.0%	34.96	0.0%
10	Staged construction model I	34.26	−0.9%	34.11	−0.9%	34.68	−0.8%
	Staged construction model II	34.31	−0.8%	34.10	−0.9%	34.75	−0.6%
	Ordinary model	55.05	0.0%	52.19	0.0%	51.01	0.0%
15	Staged construction model I	54.35	−1.3%	51.85	−0.7%	51.23	0.4%
	Staged construction model II	54.46	−1.1%	51.89	−0.6%	51.41	0.8%
	Ordinary model	76.25	0.0%	75.22	0.0%	73.48	0.0%
20	Staged construction model I	75.12	−1.5%	74.13	−1.4%	73.14	−0.5%
	Staged construction model II	75.31	−1.2%	74.22	−1.3%	73.51	0.0%
	Ordinary model	101.17	0.0%	99.80	0.0%	94.06	0.0%
25	Staged construction model I	98.73	−2.4%	97.75	−2.1%	93.85	−0.2%
	Staged construction model II	99.03	−2.1%	97.93	−1.9%	94.51	0.5%

Table 2
Results for the axial force due to dead load in a braced-bay column with a load-bearing beam (C_2) and the changes compared to the ordinary model.

Story	Model	Column axial force - C_2 (ton)					
		V braces		Inverted-V (Chevron) braces		Split-X braces	
	Ordinary model	38.22	0.0%	38.77	0.0%	37.01	0.0%
5	Staged construction model I	37.96	−0.7%	38.43	−0.9%	35.98	−2.8%
	Staged construction model II	40.52	6.0%	40.85	5.4%	40.42	9.2%
	Ordinary model	88.02	0.0%	88.01	0.0%	84.99	0.0%
10	Staged construction model I	85.85	−2.5%	85.90	−2.4%	81.55	−4.1%
	Staged construction model II	88.40	0.4%	88.22	0.2%	87.51	3.0%
	Ordinary model	150.62	0.0%	157.21	0.0%	150.72	0.0%
15	Staged construction model I	142.97	−5.1%	148.06	−5.8%	141.16	−6.3%
	Staged construction model II	146.19	−2.9%	150.53	−4.2%	146.90	−2.5%
	Ordinary model	227.15	0.0%	233.42	0.0%	225.86	0.0%
20	Staged construction model I	213.30	−6.1%	218.39	−6.4%	209.83	−7.1%
	Staged construction model II	217.16	−4.4%	220.38	−5.6%	217.05	−3.9%
	Ordinary model	310.82	0.0%	322.11	0.0%	323.44	0.0%
25	Staged construction model I	293.28	−5.6%	301.97	−6.3%	301.30	−6.8%
	Staged construction model II	297.46	−4.3%	304.53	−5.5%	308.14	−4.7%

in an internal column is primarily affected by the overall staged construction process, and the sequence of installing braces has an insignificant effect on this increase. For this purpose, the 25-story model with V braces was analyzed with different stages of construction as in the following:

(1) One story with braces built in each stage.
(2) Two stories with braces built in each stage.
(3) Three stories with braces built in each stage.
(4) Five stories with braces built in each stage.

The results obtained for the axial force in the internal column C_6

Table 3
Results for the axial force due to dead load in a braced-bay column with a non-load-bearing beam (C_5) and the changes compared to the ordinary model.

Story	Model	Column axial force - C_5 (ton)					
		V braces		Inverted-V (Chevron) braces		Split-X braces	
	Ordinary model	40.95	0.0%	41.70	0.0%	39.76	0.0%
5	Staged construction model I	41.04	0.2%	41.66	−0.1%	39.91	0.4%
	Staged construction model II	43.81	7.0%	42.93	3.0%	42.63	7.2%
	Ordinary model	92.54	0.0%	94.31	0.0%	90.15	0.0%
10	Staged construction model I	90.65	−2.0%	92.60	−1.8%	88.07	−2.3%
	Staged construction model II	94.25	1.9%	93.67	−0.7%	92.03	2.1%
	Ordinary model	153.05	0.0%	162.16	0.0%	157.43	0.0%
15	Staged construction model I	146.86	−4.0%	154.73	−4.6%	149.56	−5.0%
	Staged construction model II	150.54	−1.6%	155.84	−3.9%	154.30	−2.0%
	Ordinary model	227.28	0.0%	232.76	0.0%	234.01	0.0%
20	Staged construction model I	216.18	−4.9%	221.27	−4.9%	220.08	−6.0%
	Staged construction model II	219.71	−3.3%	221.97	−4.6%	224.67	−4.0%
	Ordinary model	315.86	0.0%	316.23	0.0%	320.88	0.0%
25	Staged construction model I	299.95	−5.0%	301.07	−4.8%	303.36	−5.5%
	Staged construction model II	304.09	−3.7%	301.82	−4.6%	308.17	−4.0%

Table 4
Results for the axial force due to dead load in an internal column with a non-load-bearing beam (C_5) and the changes compared to the ordinary model.

Story	Model	Column axial force - C_6 (ton)					
		V braces		Inverted-V (Chevron) braces		Split-X braces	
	Ordinary model	77.50	0.0%	77.97	0.0%	77.33	0.0%
5	Staged construction model I	78.11	0.8%	78.68	0.9%	78.18	1.1%
	Staged construction model II	78.13	0.8%	78.71	1.0%	78.23	1.2%
	Ordinary model	146.12	0.0%	147.31	0.0%	143.89	0.0%
10	Staged construction model I	150.63	3.1%	151.51	2.8%	149.23	3.7%
	Staged construction model II	150.71	3.1%	151.60	2.9%	149.48	3.9%
	Ordinary model	196.18	0.0%	187.57	0.0%	187.52	0.0%
15	Staged construction model I	211.07	7.6%	204.63	9.1%	204.42	9.0%
	Staged construction model II	211.35	7.7%	204.96	9.3%	205.24	9.4%
	Ordinary model	223.55	0.0%	219.14	0.0%	210.97	0.0%
20	Staged construction model I	250.11	11.9%	246.88	12.7%	241.20	14.3%
	Staged construction model II	250.65	12.1%	247.50	12.9%	242.68	15.0%
	Ordinary model	232.09	0.0%	227.43	0.0%	213.09	0.0%
25	Staged construction model I	268.49	15.7%	264.94	16.5%	252.79	18.6%
	Staged construction model II	269.14	16.0%	265.70	16.8%	254.76	19.6%

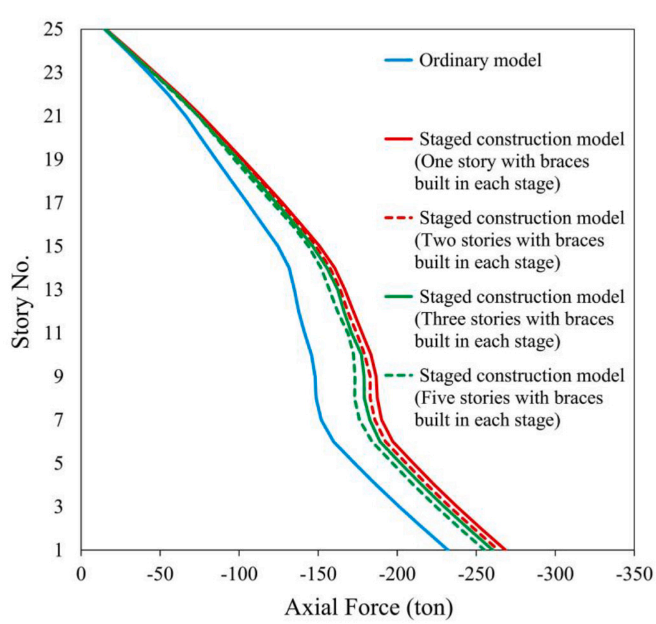

Fig. 12. Graphs of the column axial force changes for an internal column in the first story (C_6) in the 25-story model with V braces in different staged construction cases.

caused by dead load in the abovementioned model are presented in Fig. 12. As seen, with the increase in stories built during each construction stage, the effect of staged construction lessens, and the difference between the results from the staged construction and ordinary models becomes less significant.

7. Results of the pushover analyses under the AISC cyclic loading protocol

As examples, the pushover, hysteresis, and energy dissipation curves obtained for the 5- and 25-story models are presented in Figs. 13 and 14.

7.1. *The effect of staged construction on the displacement corresponding to the first plastic hinge formation*

According to the results presented in Table 5, staged construction model II increased the displacement corresponding to the first plastic hinge formation in most models. On the other hand, staged construction model I did not lead to any significant change in the abovementioned displacement. Accordingly, staged construction model II led to an increase of up to 9.3% in the displacement corresponding to the first plastic hinge formation compared to the ordinary model. Most changes corresponded to the model with split-X braces, with those with the inverted-V (Chevron) and V braces following in order. The mentioned changes decreased with the reduction in the number of stories.

In steel structures with MRF-CBF dual systems, plastic hinges are initially formed in the bracing system and, firstly, in compression braces

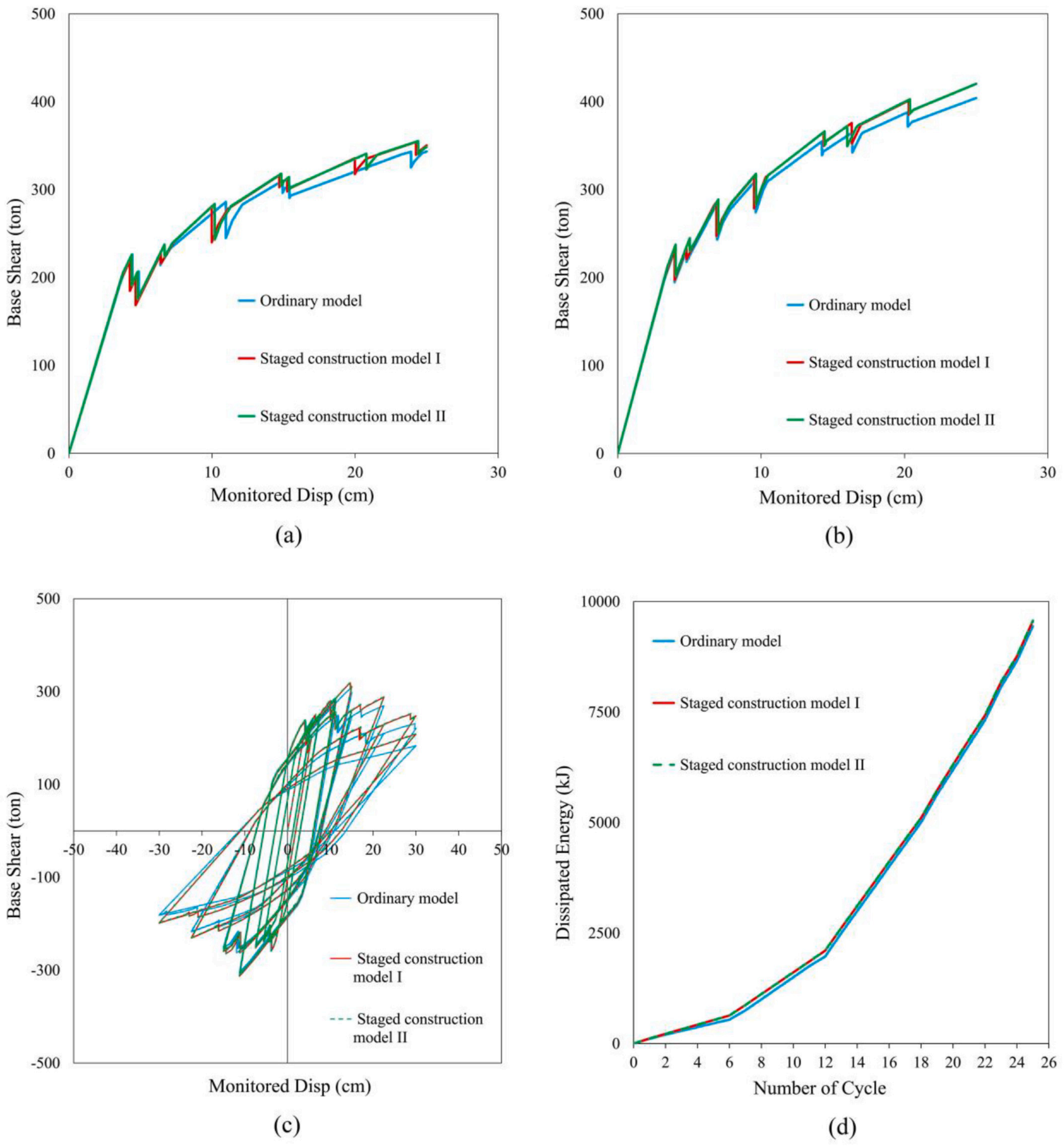

Fig. 13. Pushover and hysteresis curves for the 5-story model with V braces: (a) Pushover curves in the *X*-direction; (b) Pushover curves in the *Y*-direction; (c) Hysteresis curves in the *X*-direction; (d) Energy dissipation curves in the *X*-direction.

due to the high stiffness of the concentric braces. More specifically, a compression brace buckles due to the compressive force created in it, and the moment due to the existing compressive axial force and the deflection caused by buckling causes the formation of a moment plastic hinge in such a brace. According to the above explanation, it is evident that the reason for plastic hinge formation in compression braces is the compressive axial forces in such braces. Considering that in staged construction model II, the axial forces in the braces due to the gravity loads are practically zero, under seismic loading, the compressive axial forces in the braces are less than those in the ordinary model and staged construction model I. Accordingly, the formation of plastic hinges in the braces occurs with delay and the amount of displacement corresponding to the first plastic hinge formation in the structure increases.

The models with V, inverted-V (Chevron), and split-X braces were examined in both directions since the braced-bay beams are load-bearing in the *X*-direction but non-load-bearing in the *Y*-direction. In

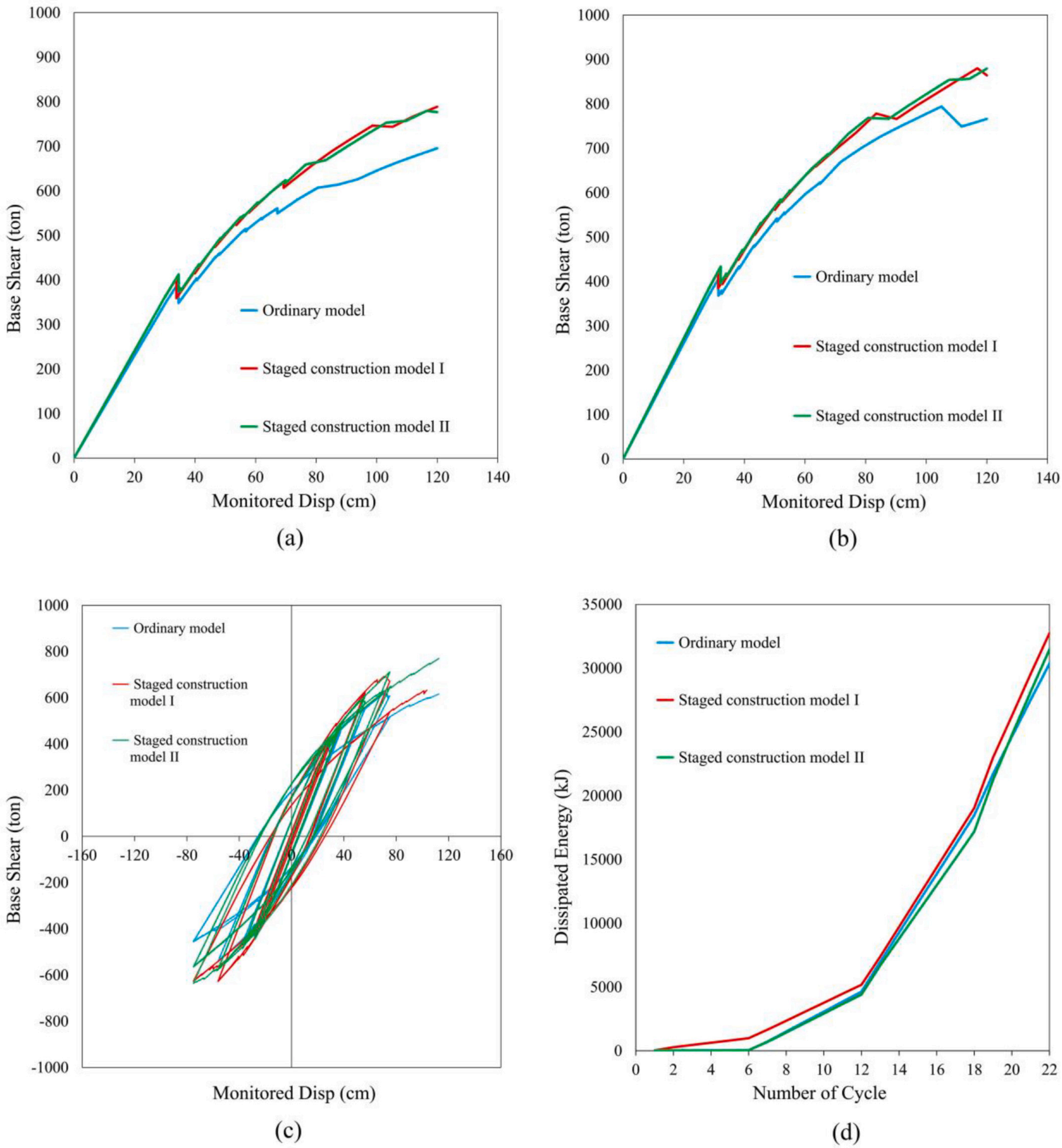

Fig. 14. Pushover and hysteresis curves for the 25-story model with V braces: (a) Pushover curves in the *X*-direction; (b) Pushover curves in the *Y*-direction; (c) Hysteresis curves in the *X*-direction; (d) Energy dissipation curves in the *X*-direction.

the ordinary model, more significant tensile axial forces are created due to the gravity loads in the *X*-direction V braces compared to the *Y*-direction ones, which have non-load-bearing braced-bay beams. As a result, in the ordinary model, the calculated compressive forces caused by gravity loads in the *Y*-direction braces are greater than those in the *X*-direction braces. As stated, the delay in the plastic hinge formation is due to the difference between the axial forces in the ordinary and staged construction models. Because this difference is more significant in the *Y*-direction braces than in the *X*-direction ones, the calculated increase in the displacement corresponding to the formation of the first plastic hinge in V braces is also greater in the *Y*-direction compared to the *X*-direction.

In accordance with the above explanations, in the ordinary model, gravity loads lead to more significant compressive axial forces in the *X*-

Table 5
Results for the displacement corresponding to the first plastic hinge formation and the changes compared to the ordinary model.

Story	Direction	Model	Displacement corresponding to the first plastic hinge formation (cm)					
			V braces		Inverted-V (Chevron) braces		Split-X braces	
5	X	Ordinary model	3.63	0.0%	2.48	0.0%	3.56	0.0%
		Staged construction model I	3.63	0.0%	2.48	0.0%	3.51	−1.4%
		Staged construction model II	3.75	3.3%	2.62	5.6%	3.70	3.9%
	Y	Ordinary model	3.26	0.0%	2.71	0.0%	3.91	0.0%
		Staged construction model I	3.25	−0.3%	2.72	0.4%	3.93	0.5%
		Staged construction model II	3.46	6.1%	2.79	3.0%	4.12	5.4%
10	X	Ordinary model	8.72	0.0%	9.54	0.0%	9.63	0.0%
		Staged construction model I	8.47	−2.9%	9.51	−0.3%	9.49	−1.5%
		Staged construction model II	8.62	−1.1%	9.92	4.0%	10.15	5.4%
	Y	Ordinary model	8.06	0.0%	8.57	0.0%	8.72	0.0%
		Staged construction model I	8.04	−0.2%	8.57	0.0%	8.76	0.5%
		Staged construction model II	8.20	1.7%	8.75	2.1%	9.41	7.9%
15	X	Ordinary model	13.92	0.0%	16.50	0.0%	15.75	0.0%
		Staged construction model I	13.33	−4.2%	16.40	−0.6%	15.46	−1.8%
		Staged construction model II	13.74	−1.3%	17.14	3.9%	16.56	5.1%
	Y	Ordinary model	13.33	0.0%	14.16	0.0%	15.56	0.0%
		Staged construction model I	13.33	0.0%	14.12	−0.3%	15.58	0.1%
		Staged construction model II	13.78	3.4%	14.51	2.5%	16.80	8.0%
20	X	Ordinary model	20.00	0.0%	23.27	0.0%	25.35	0.0%
		Staged construction model I	19.66	−1.7%	23.12	−0.6%	24.88	−1.9%
		Staged construction model II	20.00	0.0%	24.31	4.5%	26.67	5.2%
	Y	Ordinary model	16.34	0.0%	19.82	0.0%	21.05	0.0%
		Staged construction model I	16.27	−0.4%	19.70	−0.6%	21.05	0.0%
		Staged construction model II	16.75	2.5%	20.34	2.6%	22.83	8.5%
25	X	Ordinary model	30.33	0.0%	29.90	0.0%	31.86	0.0%
		Staged construction model I	29.62	−2.3%	29.55	−1.2%	31.18	−2.1%
		Staged construction model II	30.36	0.1%	31.09	4.0%	33.92	6.5%
	Y	Ordinary model	27.42	0.0%	25.00	0.0%	28.21	0.0%
		Staged construction model I	27.25	−0.6%	24.87	−0.5%	28.12	−0.3%
		Staged construction model II	28.07	2.4%	25.66	2.6%	30.84	9.3%

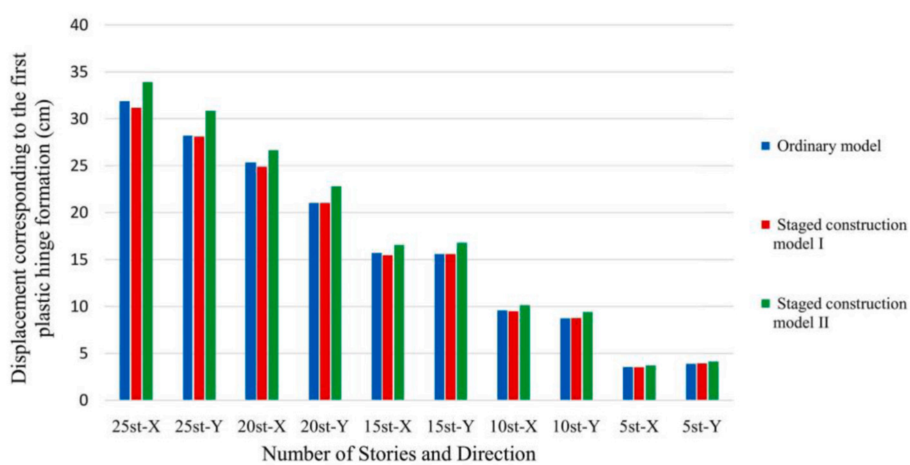

Fig. 15. Graphs of the changes in the displacement corresponding to the first plastic hinge formation in the models with split-X braces.

direction inverted-V (Chevron) braces compared to the *Y*-direction braces, which have non-load-bearing braced-bay beams. Accordingly, the calculated increase in displacement corresponding to the formation of the first plastic hinge in the inverted-V (Chevron) braces is greater in the *X*-direction than in the *Y*-direction.

Considering that in staged construction model I, the axial forces in the braces due to dead load are less than those in the ordinary model and far more than those in staged construction model II, the displacement corresponding to the first plastic hinge formation in staged construction model I was similar to the ordinary model with only a slight difference.

Fig. 15 compares the values for the displacement corresponding to the first plastic hinge formation in models with split-X braces obtained for the ordinary and staged construction models and different numbers of stories.

7.2. *The effect of staged construction on the base shear corresponding to the first plastic hinge formation*

According to the results presented in Table 6, staged construction caused an increase in the value of the base shear corresponding to the first plastic hinge formation in all models. Staged construction models I and II led to increases of respectively up to 3.4% and 13.3% in the base shear corresponding to the first plastic hinge formation compared to the ordinary model. The model with split-X braces exhibited the most

Table 6
Results for the base shear corresponding to the first plastic hinge formation and the changes compared to the ordinary model.

Story	Direction	Model	Base shear corresponding to the first plastic hinge formation (ton)					
			V braces		Inverted-V (Chevron) braces		Split-X braces	
5	X	Ordinary model	196.02	0.0%	186.69	0.0%	209.92	0.0%
		Staged construction model I	197.82	0.9%	188.09	0.7%	208.80	−0.5%
		Staged construction model II	204.36	4.3%	198.65	6.4%	219.79	4.7%
	Y	Ordinary model	197.82	0.0%	193.24	0.0%	244.22	0.0%
		Staged construction model I	199.50	0.8%	194.87	0.8%	247.39	1.3%
		Staged construction model II	212.35	7.3%	200.44	3.7%	259.22	6.1%
10	X	Ordinary model	245.95	0.0%	255.37	0.0%	249.79	0.0%
		Staged construction model I	243.35	−1.1%	259.47	1.6%	250.93	0.5%
		Staged construction model II	247.63	0.7%	270.56	5.9%	268.31	7.4%
	Y	Ordinary model	245.85	0.0%	237.75	0.0%	242.12	0.0%
		Staged construction model I	249.42	1.5%	242.00	1.8%	247.76	2.3%
		Staged construction model II	254.25	3.4%	247.17	4.0%	266.03	9.9%
15	X	Ordinary model	269.26	0.0%	296.45	0.0%	283.83	0.0%
		Staged construction model I	264.82	−1.6%	303.27	2.3%	286.66	1.0%
		Staged construction model II	272.85	1.3%	316.92	6.9%	307.13	8.2%
	Y	Ordinary model	297.15	0.0%	280.05	0.0%	315.04	0.0%
		Staged construction model I	304.14	2.4%	286.65	2.4%	323.60	2.7%
		Staged construction model II	314.33	5.8%	294.71	5.2%	348.98	10.8%
20	X	Ordinary model	316.91	0.0%	328.73	0.0%	366.21	0.0%
		Staged construction model I	321.88	1.6%	338.94	3.1%	372.47	1.7%
		Staged construction model II	327.37	3.3%	356.45	8.4%	399.20	9.0%
	Y	Ordinary model	305.24	0.0%	321.67	0.0%	356.94	0.0%
		Staged construction model I	312.69	2.4%	330.35	2.7%	367.97	3.1%
		Staged construction model II	321.87	5.4%	341.07	6.0%	399.05	11.8%
25	X	Ordinary model	349.53	0.0%	357.24	0.0%	416.85	0.0%
		Staged construction model I	357.08	2.2%	368.84	3.2%	424.40	1.8%
		Staged construction model II	365.94	4.7%	388.05	8.6%	461.78	10.8%
	Y	Ordinary model	358.25	0.0%	334.44	0.0%	412.00	0.0%
		Staged construction model I	370.53	3.4%	345.97	3.4%	425.68	3.3%
		Staged construction model II	381.71	6.5%	357.00	6.7%	466.88	13.3%

significant increase, followed by those with inverted-V (chevron) and V braces. As the number of stories decreased, the changes became less significant.

All models exhibited linear behavior prior to the formation of the first plastic hinge, with the base shear to the displacement ratio corresponding to the first plastic hinge formation equivalent to the initial lateral stiffness of the structure. On the other hand, as discussed in the previous section, results show that staged construction increased the displacement corresponding to the first plastic hinge formation. Thus, staged construction also increased the base shear corresponding to the first plastic hinge formation.

For the models with V, inverted-V (Chevron), and split-X braces, since the braced-bay beams are load-bearing in the *X*-direction and non-load-bearing in the *Y*-direction, these models were examined in both directions. Due to the gravity loads, more significant tensile axial forces are created in the *X*-direction V braces in the ordinary model compared to the *Y*-direction braces, which have non-load-bearing braced-bay beams. As a result, in the ordinary model, the calculated compressive forces in the *Y*-direction braces caused by gravity loads are more than those in the *X*-direction braces. As explained in Section 7.1, the delay in the first plastic hinge formation and the subsequent increase in the base shear corresponding to the first plastic hinge formation occurs due to the difference in the axial force in the ordinary model and staged construction model. Because this difference is more significant in *Y*-direction braces than *X*-direction braces, the calculated increase in the base shear corresponding to the first plastic hinge formation in V braces in the

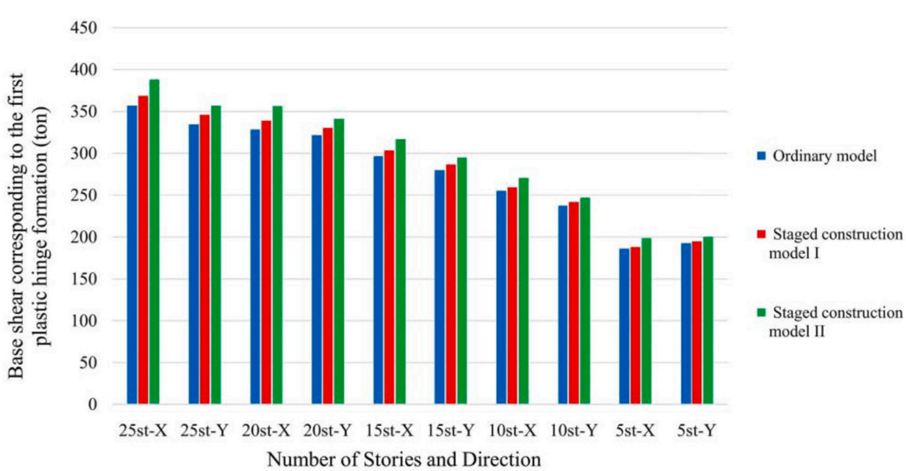

Fig. 16. Graphs of the changes in the base shear corresponding to the first plastic hinge formation in the models with inverted-V (Chevron) braces.

Table 7
Results for the ultimate lateral strength and the changes compared to the ordinary model.

Story	Direction	Model	Ultimate strength (ton)					
			V braces		Inverted-V (Chevron) braces		Split-X braces	
5		Ordinary model	343.42	0.0%	362.82	0.0%	393.09	0.0%
	X	Staged construction model I	354.20	3.1%	374.29	3.2%	407.55	3.7%
		Staged construction model II	355.31	3.5%	380.60	4.9%	408.70	4.0%
		Ordinary model	404.29	0.0%	396.42	0.0%	446.97	0.0%
	Y	Staged construction model I	420.44	4.0%	411.95	3.9%	462.26	3.4%
		Staged construction model II	420.44	4.0%	413.71	4.4%	465.50	4.1%
10		Ordinary model	435.75	0.0%	423.86	0.0%	492.53	0.0%
	X	Staged construction model I	458.90	5.3%	455.78	7.5%	521.06	5.8%
		Staged construction model II	459.74	5.5%	458.79	8.2%	520.75	5.7%
		Ordinary model	485.23	0.0%	455.72	0.0%	544.99	0.0%
	Y	Staged construction model I	517.81	6.7%	485.82	6.6%	542.81	−0.4%
		Staged construction model II	517.83	6.7%	486.89	6.8%	570.25	4.6%
15		Ordinary model	533.03	0.0%	518.14	0.0%	566.43	0.0%
	X	Staged construction model I	570.57	7.0%	560.75	8.2%	657.11	16.0%
		Staged construction model II	606.64	13.8%	556.38	7.4%	614.25	8.4%
		Ordinary model	618.27	0.0%	571.46	0.0%	588.14	0.0%
	Y	Staged construction model I	694.28	12.3%	656.07	14.8%	627.04	6.6%
		Staged construction model II	693.23	12.1%	627.85	9.9%	630.61	7.2%
20		Ordinary model	670.00	0.0%	609.65	0.0%	731.53	0.0%
	X	Staged construction model I	702.24	4.8%	718.15	17.8%	731.35	0.0%
		Staged construction model II	709.10	5.8%	677.08	11.1%	796.07	8.8%
		Ordinary model	752.34	0.0%	712.56	0.0%	704.64	0.0%
	Y	Staged construction model I	778.69	3.5%	741.60	4.1%	762.54	8.2%
		Staged construction model II	812.56	8.0%	765.64	7.4%	771.89	9.5%
25		Ordinary model	695.55	0.0%	742.90	0.0%	759.69	0.0%
	X	Staged construction model I	788.77	13.4%	787.32	6.0%	874.49	15.1%
		Staged construction model II	779.49	12.1%	818.73	10.2%	848.51	11.7%
		Ordinary model	794.09	0.0%	726.81	0.0%	891.15	0.0%
	Y	Staged construction model I	880.13	10.8%	846.16	16.4%	1075.14	20.6%
		Staged construction model II	879.52	10.8%	864.11	18.9%	1095.11	22.9%

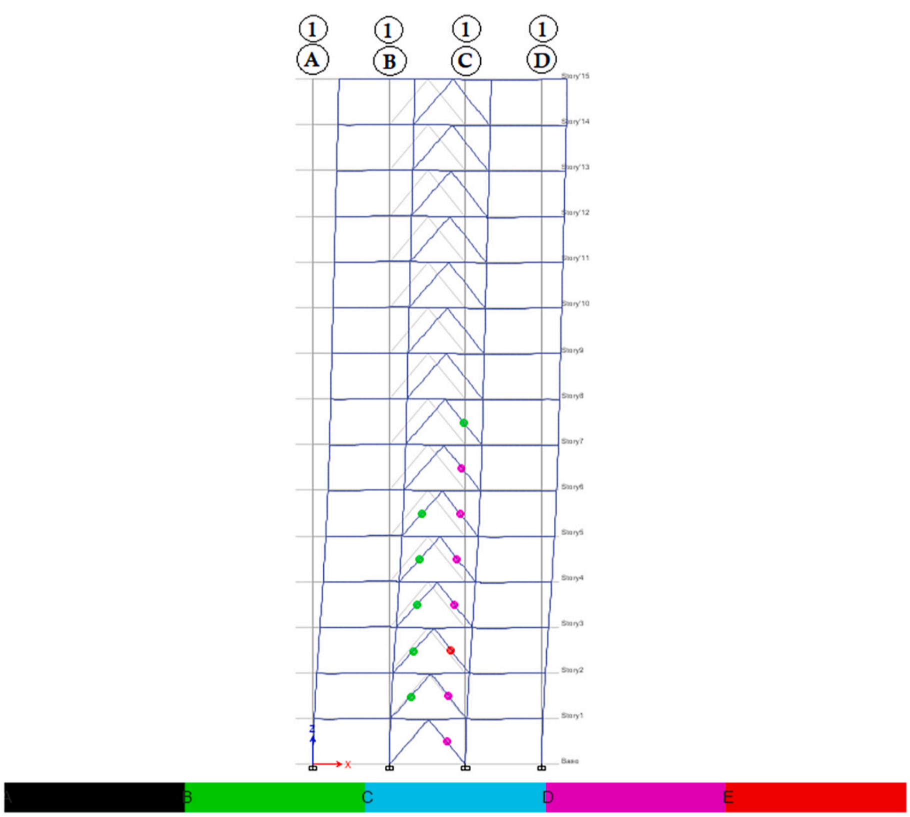

Fig. 17. Formation of plastic hinges in the 15-story model with inverted-V (Chevron) braces.

Y-direction is more than that in the *X*-direction.

According to the above explanations, in the *X*-direction inverted-V (Chevron) braces in the ordinary model, due to the gravity loads, significant compressive axial forces are created compared to the *Y*-direction braces, which have non-load-bearing braced-bay beams. Accordingly, the calculated increase in the base corresponding to the first plastic hinge formation in the inverted-V (Chevron) braces is greater in the *X*-direction compared to the *Y*-direction.

Considering that in staged construction model I, the axial forces in the braces due to dead load are less than those in the ordinary model and far more significant compared to staged construction model II, the base shear corresponding to the first plastic hinge formation, in staged construction model I was similar to the ordinary model with only a slight difference.

Fig. 16 compares the values for the base shear corresponding to the first plastic hinge formation in models with inverted-V (Chevron) braces obtained for the ordinary and staged construction models and different numbers of stories.

7.3. The effect of staged construction on the ultimate lateral strength of the structure

According to the results presented in Table 7, staged construction increased the structure's ultimate lateral strength in all models. More specifically, staged construction models I and II led to respective increases of up to 20.6% and 22.9% in the ultimate lateral strength of the structure compared to the ordinary model. The mentioned changes decreased with the reduction in the number of stories.

The sudden drops in the pushover curves presented in Figs. 13 and 14 correspond to the formation of plastic hinges in the braces in different stories and the subsequent losses of the structure's lateral strength. In the structures with MRF-CBF dual systems, the braces bear most of the lateral force due to the high stiffness of the concentric bracing system compared to the moment-resisting frame. Therefore, as seen in Fig. 17, the plastic hinges first form in the braces, causing a decrease in the structure's lateral strength.

Sen et al.'s paper [22] investigated two two-story steel frames with inverted-V (Chevron) braces and one single-story steel frame with split-X braces by conducting pushover analyses. As shown in Fig. 18, the specifications of the columns and braces were the same in all three frames, and the only difference was in the size of the braced-bay beams. The results of the pushover analyses are presented in Fig. 19. As can be seen, the resulting pushover curves also exhibit multiple sudden drops in the base shear, similar to the pushover curves obtained in this research. The reason for these drops, as stated in Sen et al.'s article, is the buckling of the braces and the formation of plastic hinges in them.

In this research, per the explanations given in the previous sections, the decrease in the axial forces caused by the gravity loads in the braces due to the effects of staged construction delayed the formation of plastic hinges in these components, which resulted in increasing the ultimate strengths of the structures analyzed.

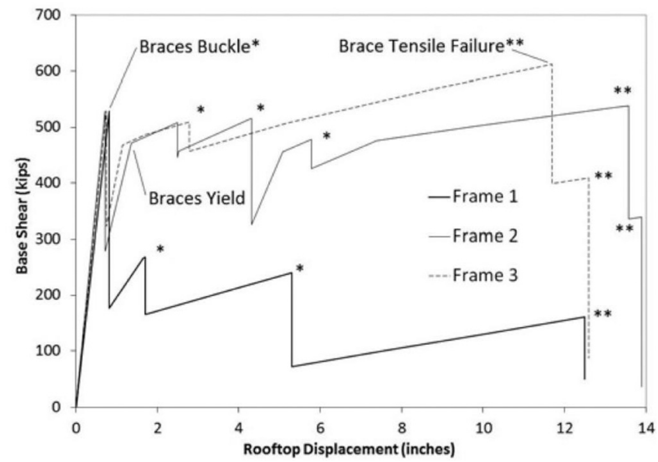

Fig. 19. Pushover curves of the frames investigated in Sen et al.'s paper [22].

Fig. 20 compares the ultimate lateral strengths obtained for the models with V braces from the ordinary and staged construction analyses.

7.4. The effect of staged construction on the effective lateral stiffness of the structure

According to the results presented in Table 8, staged construction increased the structure's effective stiffness in all models by up to 4.6% compared to the ordinary model. In addition, the mentioned changes decreased with the decrease in the number of stories.

As mentioned earlier, the effective lateral stiffness of the structure is calculated by dividing the yield base shear by the yield displacement of the structure, obtained by bilinear approximation of the pushover curve. The yield displacement and base shear in the bilinear pushover curve are affected by the area under the pushover curve, as well as the maximum displacement and base shear of the structure. As discussed, staged construction effects increase the ultimate lateral strength of the structure and, accordingly, the area under the pushover curve, causing point B in the bilinear pushover curve (Fig. 7) to have a greater height. As a result, the initial slope of the bilinear curve, which represents the effective lateral stiffness, increases.

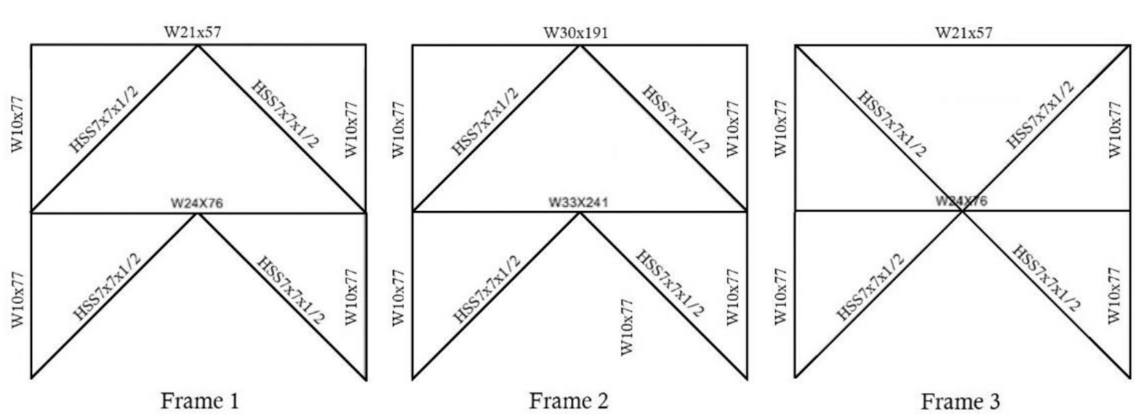

Fig. 18. Specifications of the frames investigated in Sen et al.'s paper [22].

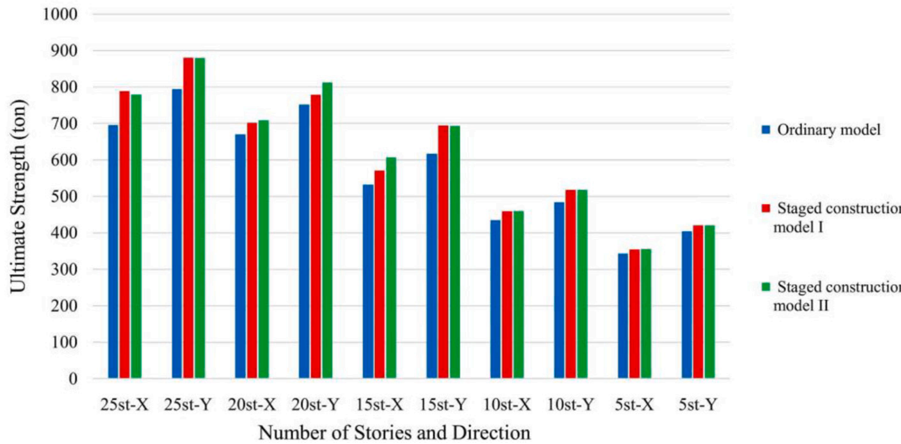

Fig. 20. Graphs of the changes in the ultimate lateral strength in the models with V braces.

Table 8
Results for the effective lateral strength and the changes compared to the ordinary model.

Story	Direction	Model	Effective stiffness - K_e (ton/cm)					
			V braces		Inverted-V (Chevron) braces		Split-X braces	
5	X	Ordinary model	53.99	0.0%	75.42	0.0%	58.94	0.0%
		Staged construction model I	54.57	1.1%	75.76	0.4%	59.48	0.9%
		Staged construction model II	54.47	0.9%	75.96	0.7%	59.49	0.9%
	Y	Ordinary model	60.75	0.0%	71.10	0.0%	62.39	0.0%
		Staged construction model I	61.35	1.0%	71.63	0.7%	62.92	0.9%
		Staged construction model II	61.27	0.9%	71.70	0.8%	62.89	0.8%
10	X	Ordinary model	28.20	0.0%	26.75	0.0%	25.93	0.0%
		Staged construction model I	28.72	1.9%	27.27	1.9%	26.44	2.0%
		Staged construction model II	28.71	1.8%	27.28	2.0%	26.44	2.0%
	Y	Ordinary model	30.48	0.0%	27.73	0.0%	27.76	0.0%
		Staged construction model I	31.00	1.7%	28.25	1.9%	28.27	1.8%
		Staged construction model II	31.00	1.7%	28.26	1.9%	28.27	1.8%
15	X	Ordinary model	19.34	0.0%	17.97	0.0%	18.03	0.0%
		Staged construction model I	19.86	2.7%	18.49	2.9%	18.54	2.9%
		Staged construction model II	19.86	2.7%	18.49	2.9%	18.54	2.8%
	Y	Ordinary model	22.29	0.0%	19.77	0.0%	20.25	0.0%
		Staged construction model I	22.81	2.4%	20.31	2.7%	20.77	2.6%
		Staged construction model II	22.81	2.4%	20.31	2.7%	20.77	2.6%
20	X	Ordinary model	15.85	0.0%	14.13	0.0%	14.45	0.0%
		Staged construction model I	16.37	3.3%	14.66	3.8%	14.97	3.6%
		Staged construction model II	16.37	3.3%	14.66	3.8%	14.97	3.6%
	Y	Ordinary model	18.69	0.0%	16.23	0.0%	16.95	0.0%
		Staged construction model I	19.22	2.8%	16.76	3.3%	17.48	3.1%
		Staged construction model II	19.22	2.8%	16.76	3.3%	17.48	3.1%
25	X	Ordinary model	11.53	0.0%	11.95	0.0%	13.08	0.0%
		Staged construction model I	12.05	4.6%	12.48	4.5%	13.61	4.1%
		Staged construction model II	12.06	4.6%	12.48	4.5%	13.61	4.1%
	Y	Ordinary model	13.07	0.0%	13.38	0.0%	14.61	0.0%
		Staged construction model I	13.60	4.1%	13.91	4.0%	15.14	3.6%
		Staged construction model II	13.60	4.1%	13.91	4.0%	15.14	3.6%

On the other hand, the reason for the stiffness decrease in models is the formation of plastic hinges in structural members. As explained in Section 7.1, staged construction causes a delay in the formation of plastic hinges in the braces. Therefore, the delay in the formation of the plastic hinges increases the lateral stiffness.

Fig. 21 compares the effective lateral strengths obtained for the models with split-X braces from the ordinary and staged construction analyses.

7.5. The effect of staged construction on energy dissipation under the AISC cyclic loading

According to the modeling and analyses conducted per the AISC cyclic loading protocol and the hysteresis curves obtained and based on the results presented in Table 9, it was determined that staged construction did not have a systematic or orderly effect on energy dissipation in the models. More precisely, the differences in energy dissipation of staged construction and ordinary models under the AISC loading protocol ranged between −8.2% and + 12.2%.

8. Results of the pushover analyses under the uniform, first mode, and inverted triangle load patterns

As examples, Fig. 22 presents the pushover curves obtained for the 5- and 25-story models with inverted-V (Chevron) braces through analyses under the uniform, first mode, and inverted triangle load patterns.

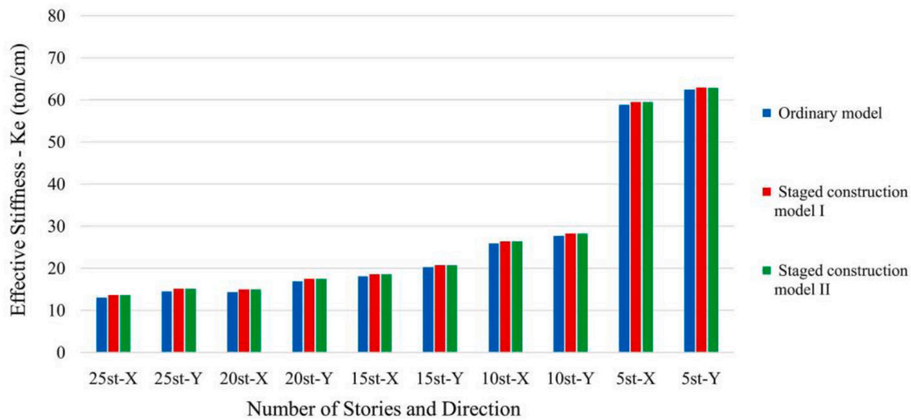

Fig. 21. Graphs of the changes in the effective lateral stiffness in the models with split-X braces.

Table 9
Results for the number of cycles and dissipated energy under the AISC loading protocol and the changes compared to the ordinary model.

Story	Direction	Model	Number of cycles and dissipated energy (kJ)								
			V braces			Inverted-V (Chevron) braces			Split-X braces		
		Ordinary model		9604	0.0%		11,665	0.0%		11,526	0.0%
5	X	Staged construction model I	25	9561	−0.4%	25	11,746	0.7%	25	10,985	−4.7%
		Staged construction model II		9568	−0.4%		12,083	3.6%		11,124	−3.5%
		Ordinary model		19,516	0.0%		16,901	0.0%		9606	0.0%
10	X	Staged construction model I	25	21,140	8.3%	25	17,396	2.9%	22	9081	−5.5%
		Staged construction model II		21,891	12.2%		17,040	0.8%		8843	−7.9%
		Ordinary model		29,747	0.0%		29,753	0.0%		23,768	0.0%
15	X	Staged construction model I	25	30,367	2.1%	26	29,306	−1.5%	24	23,999	1.0%
		Staged construction model II		30,265	1.7%		28,810	−3.2%		22,914	−3.6%
		Ordinary model		40,893	0.0%		33,937	0.0%		27,114	0.0%
20	X	Staged construction model I	25	39,630	−3.1%	25	31,829	−6.2%	23	25,417	−6.3%
		Staged construction model II		39,620	−3.1%		33,318	−1.8%		24,883	−8.2%
		Ordinary model		30,359	0.0%		34,442	0.0%		27,433	0.0%
25	X	Staged construction model I	22	32,747	7.9%	24	32,488	−5.7%	22	25,415	−7.4%
		Staged construction model II		31,472	3.7%		32,408	−5.9%		25,898	−5.6%

8.1. The effect of staged construction on the displacement corresponding to the first plastic hinge formation

Table 10 presents the results for the displacement corresponding to the first plastic hinge formation in the 5- and 25-story models obtained from pushover analyses conducted under the uniform, first mode, and inverted triangle lateral load patterns. The results presented in this table and Fig. 22 show that the values obtained for the displacement corresponding to the first plastic hinge formation were significantly higher for the first mode and inverted triangle patterns compared to those for the uniform pattern. More specifically, the results for the first mode load pattern were, on average, about 11% in 5-story models and about 46% in 25-story models, higher compared to the uniform pattern. In addition, the results of the inverted triangle pattern were, on average, 13% higher in 5-story models and 48% higher in 25-story models compared to the uniform pattern. Considering that in the 5-story models, the structure's mass participation percentage in the first mode is higher than that in the 25-story model, the results of all three models were closer to each other with less difference. The values obtained for the displacement corresponding to the first plastic hinge formation, in the cases of the first mode and inverted triangle patterns, had an average difference of about 1%, which shows that the results for these patterns were almost the same.

8.2. The effect of staged construction on the base shear corresponding to the first plastic hinge formation

Table 11 presents the results for the base shear corresponding to the first plastic hinge formation in the 5- and 25-story models, obtained through pushover analyses conducted using the uniform, first mode, and inverted triangle load patterns. From the results presented in this table and Fig. 22, it can be seen that the values calculated for the base shear corresponding to the first plastic hinge formation were significantly lower in the cases of the first mode and inverted triangle load patterns compared to the uniform load pattern. The results obtained for the first mode load pattern were, on average, about 19% lower in 5-story models and about 8% lower in 25-story models compared to the uniform load pattern. The results obtained for the inverted triangle load pattern were also, on average, about 14% lower in 5-story models and about 8% lower in 25-story models compared to the uniform load pattern. The values obtained for the base shear corresponding to the first plastic hinge formation, in the cases of the first mode and inverted triangle load patterns, had an average difference of about 3%, indicating that the results for these load patterns were almost identical.

8.3. The effect of staged construction on the final lateral strength of the structure

Table 12 presents the results for the ultimate lateral strength corresponding to the first plastic hinge formation in the 5- and 25-story

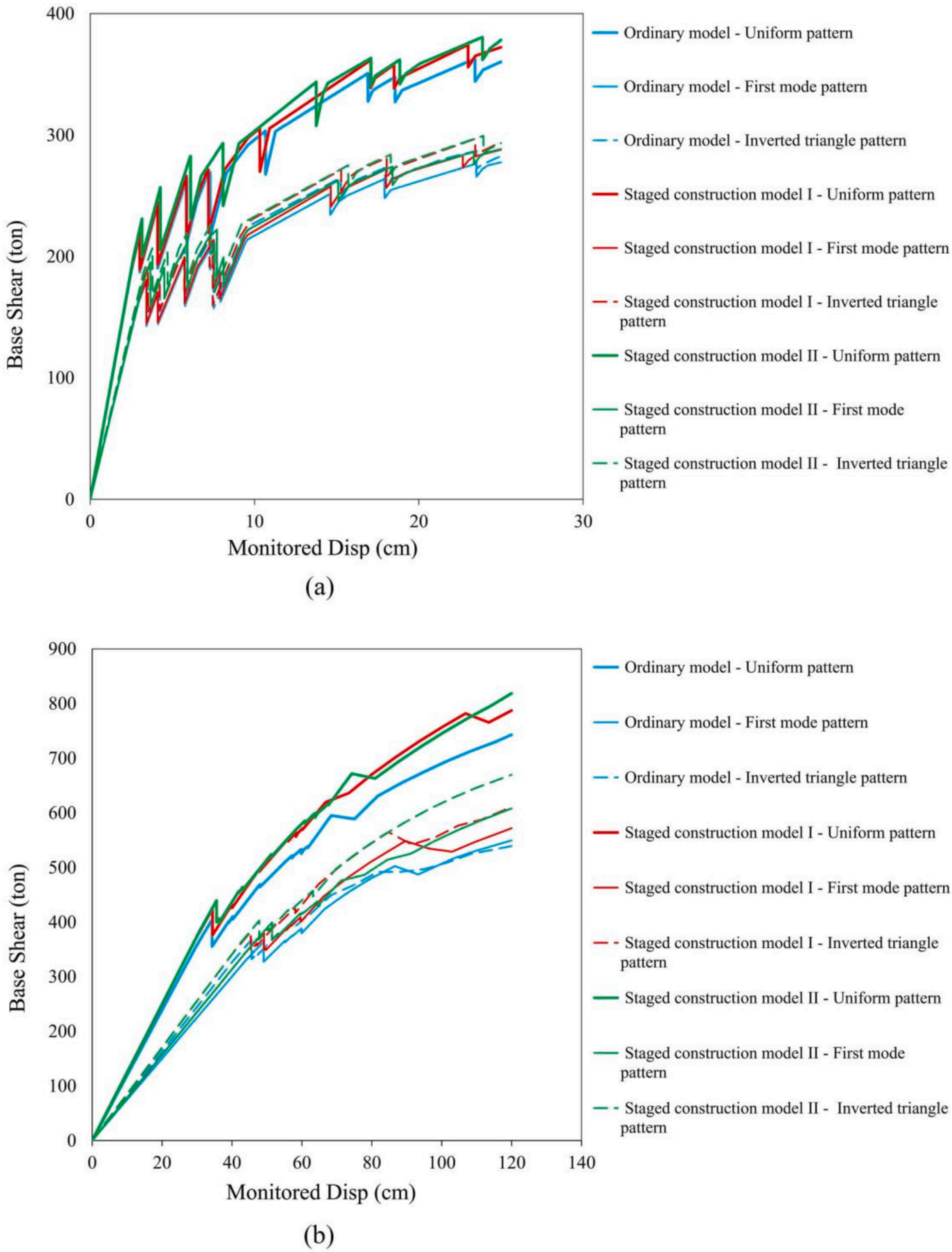

Fig. 22. Pushover curves for the 5- and 25-story models with inverted-V (Chevron) braces: (a) 5-story model in the *X*-direction; (b) 25-story model in the *X*-direction.

models, obtained through pushover analyses conducted using the uniform, first mode, and inverted triangle load patterns. From the results given in this table and Fig. 22, it is evident that the values obtained for the ultimate lateral strength of the structure were significantly lower for the first mode and inverted triangle load pattern cases compared to the uniform load pattern case. The results for the first mode load pattern were, on average, about 19% lower in 5-story models and about 20% lower in 25-story models compared to the uniform pattern. Also, the

Table 10
Results for the displacement corresponding to the first plastic hinge formation under the considered lateral load patterns.

Brace Type	Story	Direction	Model	Displacement corresponding to the first plastic hinge formation (cm)							
				Uniform pattern		First mode pattern		Inverted triangle pattern		Average	
V braces	5	X	Ordinary model	3.63	0.0%	3.88	0.0%	3.90	0.0%	3.80	0.0%
			Staged construction model I	3.63	0.0%	3.69	−4.9%	3.71	−4.9%	3.68	−3.3%
			Staged construction model II	3.75	3.3%	3.77	−2.8%	3.79	−2.8%	3.77	−0.9%
	25	X	Ordinary model	30.33	0.0%	43.41	0.0%	45.22	0.0%	39.65	0.0%
			Staged construction model I	29.62	−2.3%	42.53	−2.0%	44.32	−2.0%	38.82	−2.1%
			Staged construction model II	30.36	0.1%	43.58	0.4%	45.42	0.4%	39.79	0.3%
Inverted-V (Chevron) braces	5	X	Ordinary model	2.48	0.0%	2.93	0.0%	2.99	0.0%	2.80	0.0%
			Staged construction model I	2.48	0.0%	2.93	0.0%	2.99	0.0%	2.80	0.0%
			Staged construction model II	2.62	5.6%	3.18	8.5%	3.25	8.7%	3.02	7.7%
	25	X	Ordinary model	29.90	0.0%	43.71	0.0%	40.70	0.0%	38.10	0.0%
			Staged construction model I	29.55	−1.2%	43.69	0.0%	40.00	−1.7%	37.75	−0.9%
			Staged construction model II	31.09	4.0%	45.97	5.2%	42.72	5.0%	39.93	4.8%
Split-X braces	5	X	Ordinary model	3.56	0.0%	3.80	0.0%	3.93	0.0%	3.76	0.0%
			Staged construction model I	3.51	−1.4%	3.79	−0.3%	3.92	−0.3%	3.74	−0.6%
			Staged construction model II	3.70	3.9%	4.26	12.1%	4.26	8.4%	4.07	8.2%
	25	X	Ordinary model	31.86	0.0%	46.26	0.0%	47.60	0.0%	41.91	0.0%
			Staged construction model I	31.18	−2.1%	46.05	−0.5%	47.40	−0.4%	41.54	−0.9%
			Staged construction model II	33.92	6.5%	49.85	7.8%	51.31	7.8%	45.03	7.4%

Table 11
Results for the base shear corresponding to the first plastic hinge formation under the considered lateral load patterns.

Brace Type	Story	Direction	Model	Base shear corresponding to the first plastic hinge formation (ton)							
				Uniform pattern		First mode pattern		Inverted triangle pattern		Average	
V braces	5	X	Ordinary model	196.02	0.0%	154.15	0.0%	161.05	0.0%	170.41	0.0%
			Staged construction model I	197.82	0.9%	147.87	−4.1%	154.49	−4.1%	166.73	−2.2%
			Staged construction model II	204.36	4.3%	151.35	−1.8%	158.13	−1.8%	171.28	0.5%
	25	X	Ordinary model	349.53	0.0%	321.56	0.0%	321.07	0.0%	330.72	0.0%
			Staged construction model I	357.08	2.2%	329.27	2.4%	328.85	2.4%	338.40	2.3%
			Staged construction model II	365.94	4.7%	337.43	4.9%	337.00	5.0%	346.79	4.9%
Inverted-V (Chevron) braces	5	X	Ordinary model	186.69	0.0%	161.40	0.0%	171.15	0.0%	173.08	0.0%
			Staged construction model I	188.09	0.7%	162.56	0.7%	172.39	0.7%	174.35	0.7%
			Staged construction model II	198.65	6.4%	176.71	9.5%	187.40	9.5%	187.59	8.4%
	25	X	Ordinary model	357.24	0.0%	328.22	0.0%	332.01	0.0%	339.16	0.0%
			Staged construction model I	368.84	3.2%	342.57	4.4%	340.76	2.6%	350.72	3.4%
			Staged construction model II	388.05	8.6%	360.47	9.8%	363.94	9.6%	370.82	9.3%
Split-X braces	5	X	Ordinary model	209.92	0.0%	162.28	0.0%	175.39	0.0%	182.53	0.0%
			Staged construction model I	208.80	−0.5%	163.34	0.7%	176.54	0.7%	182.89	0.2%
			Staged construction model II	219.79	4.7%	183.42	13.0%	191.94	9.4%	198.38	8.7%
	25	X	Ordinary model	416.85	0.0%	381.31	0.0%	380.24	0.0%	392.80	0.0%
			Staged construction model I	424.40	1.8%	394.84	3.5%	393.79	3.6%	404.34	2.9%
			Staged construction model II	461.78	10.8%	427.38	12.1%	426.25	12.1%	438.47	11.6%

results for the inverted triangle load pattern were, on average, about 15% lower in 5-story models and about 20% lower in 25-story models compared to the uniform load pattern. Considering that in the 5-story models, the structure's mass participation percentage in the first mode is higher than that in the 25-story model, the results of all three models were closer to each other with less difference. The values obtained for the ultimate lateral strength, in the cases of the first mode and inverted triangle load patterns, had an average difference of about 3%, indicating that the results for these load patterns were almost identical.

8.4. The effect of staged construction on the effective lateral stiffness of the structure

Table 13 presents the results for the effective lateral stiffness of the structure in the 5- and 25-story models, obtained through pushover analyses conducted using the uniform, first mode, and inverted triangle load patterns. From the results given in this table and Fig. 22, it is evident that the values obtained for the effective lateral stiffness of the structure were significantly lower for the first mode and inverted triangle load pattern cases compared to the uniform load pattern case. The

Table 12
Results for the ultimate lateral strength under the considered lateral load patterns.

Brace Type	Story	Direction	Model	Ultimate strength (ton)							
				Uniform pattern		First mode pattern		Inverted triangle pattern		Average	
V braces	5	X	Ordinary model	343.42	0.0%	278.96	0.0%	290.22	0.0%	304.20	0.0%
			Staged construction model I	354.20	3.1%	296.14	6.2%	308.17	6.2%	319.50	5.0%
			Staged construction model II	355.31	3.5%	296.11	6.1%	308.58	6.3%	320.00	5.2%
	25	X	Ordinary model	695.55	0.0%	549.42	0.0%	544.80	0.0%	596.59	0.0%
			Staged construction model I	788.77	13.4%	610.40	11.1%	584.32	7.3%	661.16	10.8%
			Staged construction model II	779.49	12.1%	627.47	14.2%	598.28	9.8%	668.41	12.0%
Inverted-V (Chevron) braces	5	X	Ordinary model	362.82	0.0%	300.38	0.0%	310.80	0.0%	324.67	0.0%
			Staged construction model I	374.29	3.2%	317.80	5.8%	328.03	5.5%	340.04	4.7%
			Staged construction model II	380.60	4.9%	317.36	5.7%	328.08	5.6%	342.01	5.3%
	25	X	Ordinary model	742.90	0.0%	581.19	0.0%	602.37	0.0%	642.15	0.0%
			Staged construction model I	787.32	6.0%	583.51	0.4%	665.06	10.4%	678.63	5.7%
			Staged construction model II	818.73	10.2%	618.32	6.4%	679.96	12.9%	705.67	9.9%
Split-X braces	5	X	Ordinary model	393.09	0.0%	304.27	0.0%	322.79	0.0%	340.05	0.0%
			Staged construction model I	407.55	3.7%	315.57	3.7%	335.32	3.9%	352.81	3.8%
			Staged construction model II	408.70	4.0%	316.37	4.0%	334.61	3.7%	353.23	3.9%
	25	X	Ordinary model	759.69	0.0%	688.36	0.0%	609.59	0.0%	685.88	0.0%
			Staged construction model I	874.49	15.1%	734.86	6.8%	676.84	11.0%	762.06	11.1%
			Staged construction model II	848.51	11.7%	706.51	2.6%	755.56	23.9%	770.19	12.3%

Table 13
Results for the effective lateral stiffness under the considered lateral load patterns.

Brace Type	Story	Direction	Model	Effective stiffness - K_e (ton/cm)							
				Uniform pattern		First mode pattern		Inverted triangle pattern		Average	
V braces	5	X	Ordinary model	53.99	0.0%	39.77	0.0%	41.27	0.0%	45.01	0.0%
			Staged construction model I	54.57	1.1%	40.11	0.9%	41.70	1.0%	45.46	1.0%
			Staged construction model II	54.47	0.9%	40.09	0.8%	41.72	1.1%	45.43	0.9%
	25	X	Ordinary model	11.53	0.0%	7.41	0.0%	7.10	0.0%	8.68	0.0%
			Staged construction model I	12.05	4.6%	7.74	4.5%	7.42	4.5%	9.07	4.5%
			Staged construction model II	12.06	4.6%	7.74	4.5%	7.42	4.5%	9.07	4.6%
Inverted-V (Chevron) braces	5	X	Ordinary model	75.42	0.0%	57.17	0.0%	57.17	0.0%	63.25	0.0%
			Staged construction model I	75.76	0.4%	57.60	0.8%	57.60	0.8%	63.65	0.6%
			Staged construction model II	75.96	0.7%	57.56	0.7%	57.56	0.7%	63.70	0.7%
	25	X	Ordinary model	11.95	0.0%	7.51	0.0%	8.16	0.0%	9.20	0.0%
			Staged construction model I	12.48	4.5%	7.84	4.4%	8.52	4.4%	9.61	4.4%
			Staged construction model II	12.48	4.5%	7.84	4.4%	8.52	4.4%	9.61	4.4%
Split-X braces	5	X	Ordinary model	58.94	0.0%	42.69	0.0%	44.65	0.0%	48.76	0.0%
			Staged construction model I	59.48	0.9%	43.04	0.8%	45.06	0.9%	49.19	0.9%
			Staged construction model II	59.49	0.9%	43.05	0.8%	45.04	0.9%	49.19	0.9%
	25	X	Ordinary model	13.08	0.0%	8.24	0.0%	7.99	0.0%	9.77	0.0%
			Staged construction model I	13.61	4.1%	8.57	4.0%	8.31	4.0%	10.16	4.0%
			Staged construction model II	13.61	4.1%	8.56	3.8%	8.31	4.0%	10.16	4.0%

results for the first mode load pattern were, on average, about 26% lower in 5-story models and about 37% lower in 25-story models compared to the uniform pattern. Also, the results for the inverted triangle load pattern were, on average, about 24% lower in 5-story models and about 36% lower in 25-story models compared to the uniform load pattern. Considering that in the 5-story models, the structure's mass participation percentage in the first mode is higher than that in the 25-story model, the results of all three models were closer to each other with less difference. The values obtained for the effective lateral stiffness, in the cases of the first mode and inverted triangle load patterns, had an average difference of about 2%, indicating that the results for these load patterns were almost identical.

Overall, by examining the results presented in Sections 8.1 to 8.4, it can be concluded that changes resulting from the staged construction models compared to the ordinary model were almost identical in all load pattern cases. Furthermore, the average of the changes corresponding to the three load patterns presented in Tables 10 to 13 matched those obtained for the uniform load pattern used in this research. Accordingly, it seems that the lateral load pattern does not significantly affect the changes in the amount of the investigated parameters, namely the

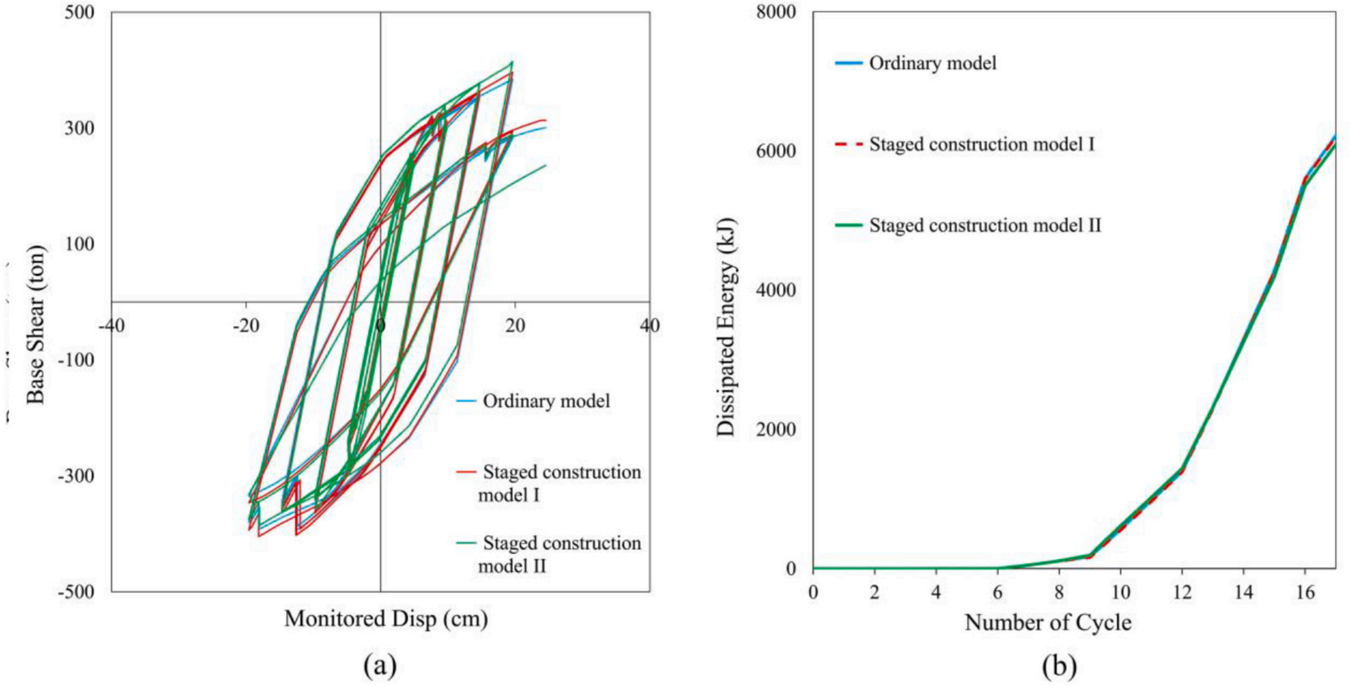

Fig. 23. Hysteresis and energy dissipation curves for the 5-story model with split-X braces: (a) Hysteresis curves in the *X*-direction; (b) Energy dissipation curves in the *X*-direction.

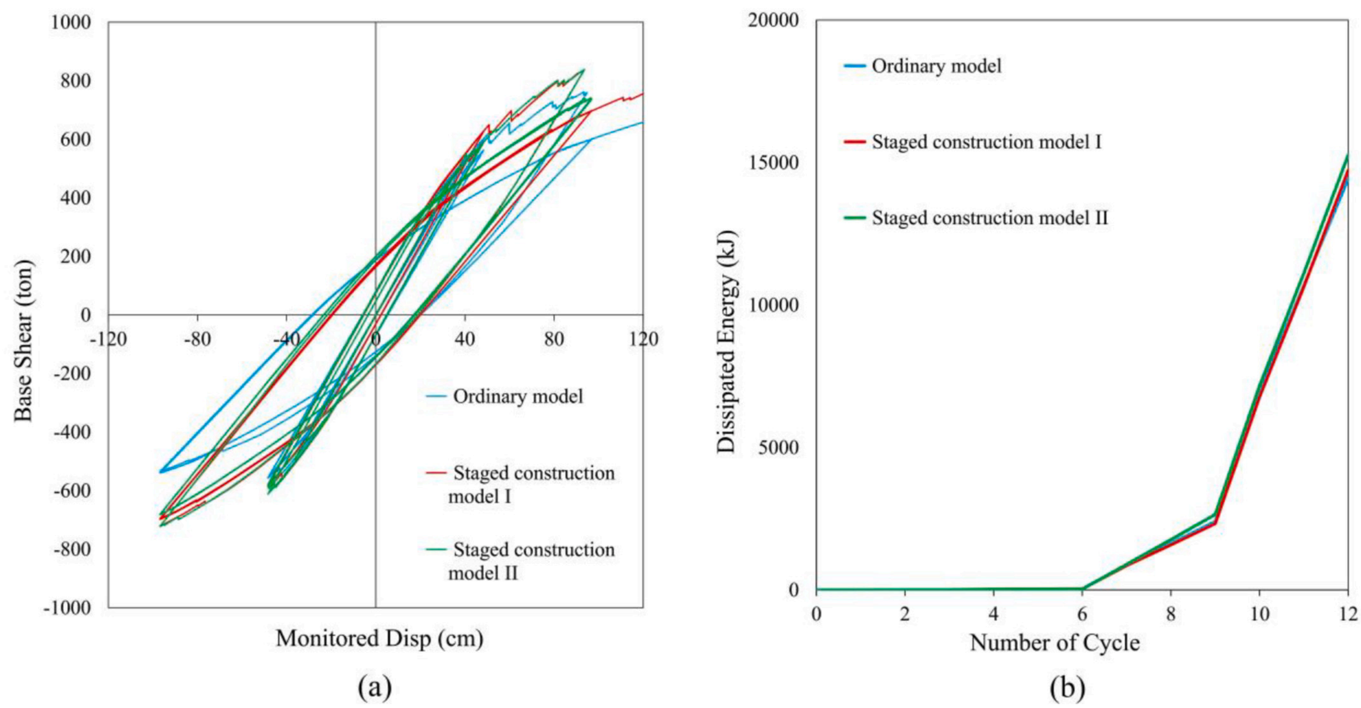

Fig. 24. Hysteresis and energy dissipation curves for the 25-story model with split-X braces: (a) Hysteresis curves in the *X*-direction; (b) Energy dissipation curves in the *X*-direction.

displacement and base shear corresponding to the first plastic hinge formation, ultimate lateral strength, and effective lateral stiffness, resulting from staged construction compared to the ordinary analysis model.

9. Results of analysis under the ATC-24 cyclic loading protocol

According to the modeling and analyses conducted under the ATC-24 cyclic loading protocol, the hysteresis curves obtained (examples for the 5- and 25-story models with split-X braces given in Figs. 23 and 24), and also the results presented in Table 14, it was determined that stage

Table 14
Results for the number of cycles and dissipated energy under the ATC-24 loading protocol and the changes compared to the ordinary model.

Story	Direction	Model	Number of cycles and dissipated energy (kJ)								
			V braces			Inverted-V (Chevron) braces			Split-X braces		
		Ordinary model		4754	0.0%		4589	0.0%		6217	0.0%
5	X	Staged construction model I	19	5142	8.2%	17	4576	−0.3%	17	6200	−0.3%
		Staged construction model II		5078	6.8%		4494	−2.1%		6093	−2.0%
		Ordinary model		14,949	0.0%		12,349	0.0%		15,219	0.0%
10	X	Staged construction model I	19	15,735	5.3%	19	12,404	0.4%	19	14,871	−2.3%
		Staged construction model II		15,241	2.0%		12,495	1.2%		14,818	−2.6%
		Ordinary model		27,341	0.0%		28,530	0.0%		25,303	0.0%
15	X	Staged construction model I	18	26,846	−1.8%	19	27,910	−2.2%	17	25,683	1.5%
		Staged construction model II		26,801	−2.0%		27,458	−3.8%		25,982	2.7%
		Ordinary model		7944	0.0%		28,837	0.0%		21,851	0.0%
20	X	Staged construction model I	12	7644	−3.8%	17	27,762	−3.7%	15	20,882	−4.4%
		Staged construction model II		7774	−2.1%		28,572	−0.9%		20,697	−5.3%
		Ordinary model		33,879	0.0%		28,390	0.0%		14,437	0.0%
25	X	Staged construction model I	15	32,310	−4.6%	15	27,140	−4.4%	12	14,726	2.0%
		Staged construction model II		32,244	−4.8%		27,202	−4.2%		15,259	5.7%

construction did not have any systematic or orderly effect on energy dissipation in the models. More precisely, the calculated changes in the amount of energy dissipation resulting from the staged construction models compared to the ordinary model ranged between −5.3% and + 8.2%.

In the ATC-24 cyclic loading protocol, unlike the AISC loading protocol, the displacement applied to the structure is based on the displacement corresponding to the yield point of the structure. Hence, in this protocol, the displacement applied is proportional to the lateral stiffness of the structure. Therefore, almost all models with different numbers of stories enter the non-linear range in a certain cycle.

10. Conclusion

According to the explanations and interpretation provided in the previous sections, the findings of this study regarding the effects of staged construction on structures with dual MRF-CBF systems can be summarized as follows:

(1) In an internal column (C_6), staged construction increased the axial force due to dead load up to 19.6%. According to the case study conducted, a 19.6% increase in the axial forces caused by dead load can lead to an increase of about 12% in the DCR of an internal column under the critical design load combination. Therefore, when the effects of staged construction are not considered, the design force corresponding to an internal column is estimated to be less than the actual amount. Such an issue leads to incorrect design, which can be dangerous. Furthermore, the amount of increase in the mentioned axial force decreases with the decrease in the number of stories. The most significant increase in the axial force due to dead load in an internal column (C_6) resulting from the effects of staged construction was observed in the models with split-X braces, with those with inverted-V (Chevron) and V braces following in order.

(2) The effect of staged construction on the axial forces caused by dead load in corner columns (C_1), braced-bay columns with load-bearing beams (C_2), and braced-bay columns with non-load-bearing beams (C_5) was found to be insignificant and thus can be ignored. Also, in most models, staged construction was found to reduce the axial forces in the mentioned column types due to dead load, which can be considered in the direction of reliability.

(3) Staged construction model II led to an increase in the displacement corresponding to the first plastic hinge formation in almost most models. More specifically, staged construction model II resulted in up to a 9.3% increase in the displacement corresponding to the first plastic hinge formation compared to the ordinary model. The most significant changes were respectively related to the models with split-X braces, with those with inverted-V (Chevron) and V braces following in order. The mentioned changes decreased with the reduction in the number of stories.

(4) Staged construction caused an increase in the base shear corresponding to the first plastic hinge formation in all models. More specifically, staged construction models I and II, respectively, led to increases of up to 3.4% and 13.3% in the base shear corresponding to the first plastic hinge formation compared to the ordinary model. The most significant changes were respectively related to the models with split-X braces, with those with inverted-V (Chevron) and V braces following in order. The mentioned changes decreased with the reduction in the number of stories.

(5) Staged construction increased the ultimate strength of the structure in all models. More precisely, staged construction models I and II, respectively, resulted in increases of up to 20.6% and 22.9% in the ultimate strength of the structure compared to the ordinary model. The mentioned changes decreased with the reduction in the number of stories.

(6) Staged construction increased the effective stiffness of the structure in all models by up to 4.6% compared to the ordinary model. The mentioned changes decreased with the reduction in the number of stories.

(7) Staged construction was not found to have a systematic or orderly effect on the energy dissipation of the models under cyclic loading protocols. More precisely, the resulting changes varied between −8.2% and + 12.2% under the AISC cyclic loading protocol and between −5.3% and + 8.2% under the ATC-24 cyclic loading protocol compared to the ordinary model.

Declaration of Competing Interest

The authors whose names are listed immediately below certify that they have no affiliations with or involvement in any organization or entity with any financial interest (such as employment, patent-licensing arrangements, etc.), or non-financial interest (such as personal or professional relationships, affiliations, knowledge or beliefs) in the subject matter discussed in this manuscript.

Data availability

The data that has been used is confidential.

References

[1] S. Panigrahi, V. Patil, S.H. Madan, S. Takkalaki, Importance of construction sequence analysis in design of high rise building, IJISET-Int. J. Innov. Sci. Eng. Technol. 6 (2019) 1–9.
[2] M. Dinar, M. Rasel, A. Chowdhury, Ashraf, chronological construction sequence effects on reinforced concrete and steel buildings, Int. J. Eng. Sci. 3 (2014) 52–63.
[3] C. Choi, E. Kim, Multistory frames under sequential gravity loads, J. Struct. Eng. 111 (1985) 2373–2384, https://doi.org/10.1061/(asce)0733-9445(1985)111:11(2373).
[4] Computers and Structures, Inc. (CSI), ETABS | Integrated Building Analysis Design Software, Computers and Structures Inc, Berkeley, CA, 2016.
[5] G. Girija Das, K.I. Praseeda, Comparison of conventional and construction stage analysis of a RCC building, IJSTE - Int. J. Sci. Technol. Eng. 3 (2016) 50–57.
[6] J.V.G. Rao, D. Ramesh Babu, M. Selvan, V. Kiran Kumar, Study and comparison of construction sequence analysis with regular analysis by using E-TABS, Civ. Eng. Inter. J.[CEIJ] TM. 2 (2016).
[7] S.R. Amin, S.K. Mahajan, Analysis of multi storied Rcc building for construction sequence loading, Int. J. Mod. Trend Eng. Res. (2015) 2–4.
[8] T.G. Shirhatti, S.B. Vanakudre, The effects of P-delta and construction sequential analysis of RCC and steel building with respect to linear static analysis, Int. Res. J. Eng. Technol. 2 (2015) 501–505.
[9] R. Pranay, I.Y. Sreevalli, S. Kumar, Study and comparison of construction sequence analysis with conventional lumped analysis using ETABS, Int. J. Sci. Eng. Technol. Res. 10 (2021) 16–27.
[10] V.S.R. Jagarlamudi, K. Manoj, ISSN no : 2348-4845 study and comparison of sequence analysis with conventional lumped analysis using ETABS, Int. J. Mag. Eng. Technol. Manag. Res. 2 (2015) 265–268.
[11] K.M. Pathan, S.W. Ali, H.T. Khan, M.S. Mirza, M. Waseem, S. Zubair, Construction stage analysis of RCC frames, Int. J. Eng. Technol. Res. (2014) 54–58.
[12] D. Rodríguez, E. Brunesi, R. Nascimbene, Fragility and sensitivity analysis of steel frames with bolted-angle connections under progressive collapse, Eng. Struct. 228 (2021), 111508, https://doi.org/10.1016/j.engstruct.2020.111508.
[13] K.K. Wijesundara, R. Nascimbene, G.A. Rassati, Evaluation of the seismic performance of suspended zipper column concentrically braced steel frames, J. Constr. Steel Res. 150 (2018) 452–461, https://doi.org/10.1016/j.jcsr.2018.09.003.
[14] V. Mazzotta, E. Brunesi, R. Nascimbene, Numerical modeling and seismic analysis of tall steel buildings with braced frame systems, Period. Polytech. Civ. Eng. 61 (2017) 196–208, https://doi.org/10.3311/PPci.9469.
[15] K.K. Wijesundara, G.A. Rassathi, R. Nascimbene, D. Bolognini, Seismic performance of brace-beam-column connections in concentrically braced frames, Struct. Congr. 2010 (2010) 930–942, https://doi.org/10.1061/41130(369)85.
[16] AISC, Minimum Design Loads for Buildings and Other Structures, ASCE7–16, 2016.
[17] AISC, Specification for Structural Steel Buildings, ANSI/AISC360-10, American Institute of Steel Construction, Chicago, 2010.
[18] AISC, Seismic Provisions for Structural Steel Buildings, ANSI/AISC 341-10., American Institute of Steel Construction, Chicago, 2010.
[19] Prestandard and commentary for the seismic rehabilitation of buildings, FEMA 356.
[20] ATC-24., Guidelines for Cyclic Testing of Components of Steel Structures 11, Applied Technology Council, Redwood City, CA, 1992.
[21] P. Panyakapo, Cyclic pushover analysis procedure to estimate seismic demands for buildings, Eng. Struct. 66 (2014) 10–23.
[22] A.D. Sen, C.W. Roeder, D.E. Lehman, J.W. Berman, C. Roeder, How big is that beam, Struct. Mag. (2010) 27–29.